» I've lost control again
And how I'll never know just why or understand, she said
I've lost control again
And she screamed out, kicking on her side and said
I've lost control again «[1]

6. Living Radical Polymerization in Miniemulsion using Reversible Addition–Fragmentation Chain Transfer.[2]

Synopsis: In theory, a miniemulsion comprises the ideal environment for 'living' radical polymerization by the RAFT process. Compartmentalization minimizes radical–radical termination events and droplet nucleation eliminates the mass transfer limitations found in conventional 'living' emulsion polymerizations as discussed in the previous chapter. In practice, however, several phenomena were observed when using the RAFT technique indicating a deviation from this idealized theory when the miniemulsion was stabilized by ionic surfactants. The appearance of a separate organic phase after initiation was an obvious indicator of droplet instability. The generation of oligomers in the early stages of the polymerization was postulated as the major culprit behind the destabilization. The application of nonionic surfactants allowed the controlled polymerization of methacrylates and styrene monomers, resulting in stable colloidal dispersions. The living character of this latex material was further exemplified by its transformation into block copolymers. The increased polymerization rate of the compartmentalized system allowed for improved block copolymer purity compared to homogeneous systems.

6.1. Miniemulsions

6.1.1. Introduction

Miniemulsions differ from emulsions solely in the 'mini' prefix. 'Mini' in this case refers to the monomer droplet size of the emulsion before polymerization and not to the particle size of the dispersion generated after polymerization. This

droplet size can be up to an order of magnitude smaller than in a macroemulsion or conventional emulsion.* In a typical macroemulsion polymerization, the diameter of the monomer droplets falls between one and ten micrometer at the start of the reaction,[3,4] while in a miniemulsion polymerization, the droplet size can range from an approximate 50 nm to around 500 nm.[5] Section 6.1.2 demonstrates how emulsions with such small droplets are prepared and how they are stabilized. Although mere size seems a rather arbitrary classification, the reduction in size together with the different method of preparation has some important consequences for the distribution of surfactant in the system, thereby impacting upon the nucleation mechanism (section 6.1.3, page 139).

This chapter describes the application of RAFT in miniemulsions with the aim to conduct a living polymerization. The highlight in sections 6.2 and 6.3 is on unforeseen phenomena observed involving destabilization of the miniemulsion due to the presence of the RAFT agent, when it was stabilized by either anionic or cationic surfactants. In section 6.4 these deleterious effects will be shown to be alleviated by substituting nonionic for ionic surfactants, thereby allowing the preparation of homopolymers and block copolymers with a 'livingness' unequalled by homogeneous systems.

6.1.2. Miniemulsion Preparation & Stability

The small droplets of a miniemulsion are actualized through ultra-high shear, usually by probe-sonication of the emulsion, and during this preparation a steady state droplet size is obtained after a certain minimum energy input. This equilibrium droplet size depends on the relative amounts of water, organic materials and surfactant. At this point, the rate of droplet fission by ultrasound balances the rate of droplet coalescence due to insufficient colloidal stability while thermodynamic aspects are of lesser importance during this stage.[6] When the energy input of the sonicator probe is stopped, the miniemulsion leaves its steady state situation and the droplets will slowly start growing as a result of insufficient thermodynamic and colloidal stability.

The colloidal stability is poor because of the incomplete surface coverage of the droplets with surfactant. Landfester *et al.* showed that the average droplet size of miniemulsions that are not polymerized, slowly increases to a certain plateau

* The remainder of this chapter will utilize the term 'macroemulsion' to refer to a conventional emulsion in order to emphasize the difference with miniemulsions.

value, the height of which is relatively independent of the initial droplet size.[6] In this final state the total interfacial area between the two phases has decreased to such a level that the available surfactant is able to provide the required colloidal stability. The addition of a small amount of surfactant right after the preparation of a miniemulsion effectively stops the tendency for the droplets to grow as the surface coverage with surfactant is completed. The addition of an excess surfactant, on the other hand, has an adverse effect. Free surfactant in the water phase increases the solubility of the organic material in the continuous phase which accelerates destabilization on thermodynamic grounds[7,8] and when polymerizing, free surfactant will promote secondary nucleation. The nucleation mechanism is discussed in section 6.1.3 on page 139.

Thermodynamically, the stability would be unsatisfactory if only a surfactant were applied to stabilize the droplets. This is caused by the Ostwald ripening process, which in general terms describes the effect that larger bodies tend to grow at the expense of smaller ones through diffussion of material. The effect is known to occur in aggregations of crystals for instance, but in the case of miniemulsions the bodies refer to the emulsion droplets. The effect is founded on the principle that the chemical potential of the material near an interface is higher than that of an imaginary interface-free bulk phase. The difference in chemical potential ($\Delta\mu$) between droplet material (μ_d) and bulk material (μ_b) is given by the Laplace pressure that takes the form of Eq. 6-1 for spherical liquid droplets:[9]

$$\Delta\mu = \mu_d - \mu_b = \frac{2 \cdot \sigma \cdot v_b}{r} \qquad \textbf{(6-1)}$$

where σ is the surface tension of the liquid–liquid interface, v_b is the volume of a single molecule and r the radius of the droplet. Considering the dependency of $\Delta\mu$ on r in Eq. 6-1, there will be a driving force for material to migrate from the smaller droplets to the larger droplets, attaining a state of lower energy until eventually $\Delta\mu$ is minimized. The smaller droplets will vanish as their contents diffuse to the larger ones finally resulting in the formation of a ‘single droplet’ or, in other words, complete phase separation. A somewhat lower surface energy introduced by the surfactant may reduce the rate of the process slightly but cannot prevent it.

Miniemulsions gain their stability from the addition of an extra component to the droplet phase.[7,10] Traditionally hexadecanol was used as a cosurfactant resulting in prolonged stability periods stretching from days to months. Its advantageous

effect was believed to originate from a rigid, structured complex formed by interaction of the hydrophobic tails of the surfactant (typically a long chain alkyl sulfate like dodecyl sulfate) with those of the cosurfactant, which would form an electrostatically charged barrier, decelerating monomer diffusion and, in addition, improving the colloidal stability. At present, completely hydrophobic materials like hexadecane,[10] dodecyl mercaptan[11] and stearyl methacrylate[12] often replace the cosurfactant as these were found to work even better. It is unlikely that these hydrophobic molecules will reside in the surfactant layer and the effectiveness of these costabilizers* is based on the osmotic pressure that they introduce to (partly) counterbalance the Laplace pressure, effectively minimizing the driving force for Ostwald ripening. This effect is quantified in Eq. 6-2 through the addition of an additional term on the right hand side:[9]

$$\Delta\mu = \mu_b - \mu_d = \frac{2 \cdot \sigma \cdot v_b}{r} - \frac{\eta \cdot k_B \cdot T \cdot v_b}{(4\pi/3) \cdot r^3} \qquad \textbf{(6-2)}$$

where η equals the number of hydrophobe molecules inside a particle, k_B is Boltzmann's constant and T is the absolute temperature. The total free energy of the system is found by integration of the chemical potential over all material, *i.e.* over all droplets of all volumes. The presence of the costabilizer molecules adds an important constraint on the minimization of the total free energy, namely that of a constant number of droplets. For if the costabilizer molecules are equally distributed over all droplets and approximately insoluble in the continuous phase, then the droplets initially formed cannot disappear completely by monomer depletion. In fact, should a number of large droplets expand at the expense of the smaller ones, then the osmotic pressure term for the small droplets rapidly becomes larger as r decreases, but due to the hydrophobe molecules, the system cannot be relieved of the small, high energy droplets. Strictly speaking, the Eq. 6-2 is no longer valid when the costabilizer molecules can no longer be considered 'dilute', but the formula reasonably indicates the trend in chemical potential when r decreases.

* In the current literature the term 'costabilizer' is used interchangably with 'hydrophobe' and sometimes 'cosurfactant' is still used. Though hydrophobicity is an important prerequisite for costabilizers, other aspects like solubility in the organic phase and molar masss have an important influence on their effectiveness as costabilizers. The term 'cosurfactant' is no longer indicative of the underlying mechanism of operation but seems to be adopted by some researchers and used for consistency with older literature.

Eq. 6-3 indicates that for a certain concentration of costabilizer, a droplet size exists that is thermodynamically stable. For this idealized picture to be realized in practice, it is of the utmost importance that the hydrophobe is completely insoluble in the water phase. If not, then η cannot be considered constant and the diffusion rate of the hydrophobe through the water phase is the rate determining step for the Ostwald ripening process. Since the *number* and not the *concentration* of hydrophobic species within each droplet determines its chemical potential, it is crucial that a (close to) monodisperse distribution of droplets is prepared from the homogeneous solution of costabilizer in monomer. A tailed particle size distribution containing a fraction of large droplets creates a complex situation with a similar distribution in η among the droplets, introducing a substantial driving force for interparticle monomer migration.

$$r = \left(\frac{3 \cdot \eta \cdot k_B \cdot T}{8\pi \cdot \sigma} \right)^{0.5} \qquad \textbf{(6-3)}$$

Larger hydrophobic species like polystyrene and poly(methyl methacrylate) have also been used to improve the particle stability causing higher reaction rates and a more robust nucleation process.[13,14,15] The mechanism behind their functioning is not clear, but in the light of the previous discussion it can be said that these polymers will not form very efficient costabilizers in the thermodynamic sense as their high molar mass results in a low number of molecules (η) per droplet when only a limited amount on a weight basis is used. Like their low molar mass counterparts, these polymers will fix the number of droplets as their presence prevents the disappearance of any droplets.

6.1.3. Nucleation Processes

In a macroemulsion, the surface area of the monomer phase is rather small because of the large droplet size and the consequently smaller number of droplets (typically 10^{13}dm^{-3}). The surfactant micelles, small in size (5 to 10 nm) and large in number (typically 10^{20}dm^{-3}), have a surface area that easily exceeds that of the monomer droplets.[4] For this reason, in a typical macroemulsion polymerization, micellar nucleation is the predominant mechanism for particle formation. Oligomer radicals – generated in the water phase – enter micelles and continue growing while

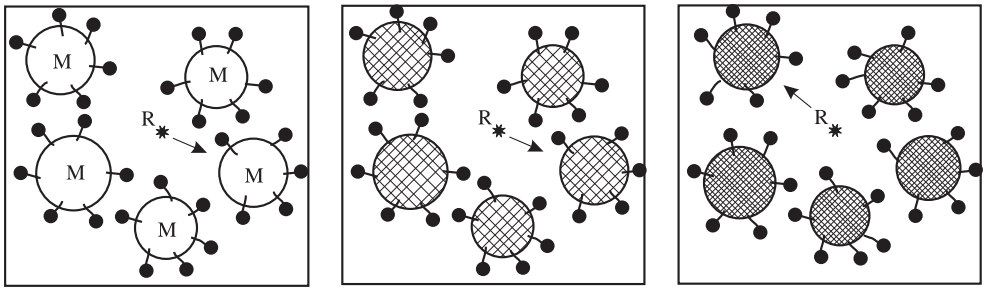

Scheme 6.1. Schematical progress of a miniemulsion polymerization. Compared with Scheme 5.3 on page 111, which represents a conventional emulsion polymerization, the starting situation of a miniemulsion polymerization is characterized by the absence of micelles in the continuous phase and by monomer droplets, that are typically larger in number and smaller in size. Particles are formed by polymerization taking place within these droplets eliminating the need for monomer migration through the continuous phase.

attracting monomer. As the micelles are converted into polymer particles, all of the reaction ingredients (*e.g.* monomer) have to migrate out of the droplets, through the water phase, into the growing particles.

In miniemulsions, the smaller droplet size has some important consequences for the course of the reaction. The smaller droplets share a much larger interphase with the continuous phase and absorb most of the surfactant in the recipe. This leaves little or no surfactant for the formation of micelles. Both the absence of micelles and the increased surface area of the droplet phase promote droplet nucleation and eliminate micellar nucleation. Oligomer radicals that are formed in the water phase enter droplets and start polymerization within them. Under these circumstances the droplets *themselves* are converted into polymer particles[16] and transport of monomer and other reaction components through the water phase is not necessary. In the ideal case, the droplets act completely independent and can be considered a collection of nanoscale bulk reactors. For this reason the resulting polymer dispersion is a copy of the initial emulsion in terms of particle size, number and identity (Scheme 6.1).[5]

Several factors may cause reality to deviate from this idealized situation. First, the presence of additional nucleation mechanisms cannot be ruled out completely. Although micellar nucleation is unlikely, due to the low free surfactant concentration, homogeneous nucleation has been shown to lead to the formation of new particles.[17,18] Homogeneous nucleation is a particle formation mechanism that takes place when an oligomeric radical in the water phase does not enter a droplet or micelle, but propagates till it reaches a critical chainlength (j_{crit}), upon which it is

no longer dissolved in the waterphase. Its coil collapses at this point, excluding water and attracting monomer thereby forming a new particle. The extent to which this occurs depends on numerous factors, the most important being the number of droplets, the amount of monomer in the water phase, the propagation rate constant in the waterphase and the type of initiator used.

Second, not all droplets may be converted into particles. It was shown in the previous section that a typical miniemulsion finds itself in a metastable situation. The chemical potential of the droplet material may be higher than that of a bulk phase but the difference is minimized through the addition of a costabilizer and all droplets share the same osmotic pressure. The difference in osmotic pressure among the droplets will be increased however, when in the course of the reaction some are nucleated while others are not. The droplets lacking polymer will eventually supply monomer to the reacting polymer particles and act as monomer reservoirs.

To fully enjoy the benefits of miniemulsion polymerization, *i.e.* completely eliminating mass transfer through the water phase, it is important to closely approach the situation of complete and exclusive droplet nucleation. This is of particular importance for living radical polymerizations as will be shown in the next section.

6.1.4. Living Radical Polymerization in Miniemulsions

In the previous chapter it was already mentioned that a major challenge confronting living radical polymerization is its application in dispersed media; most notably in water-borne systems. While macroemulsion polymerization is beyond any doubt the most straightforward approach to obtain water based polymeric dispersions, the previous chapter demonstrated that the application of RAFT in these systems resulted in unforeseen problems, even though a living mechanism based on reversible transfer was expected to be the most easily adaptable. In principle, the miniemulsion environment should allow the ideal conditions for living radical polymerization to be attained in a more straightforward manner. Similar to macroemulsion polymerization, irreversible radical–radical termination is minimized through compartmentalization, thereby allowing a higher polymerization rate compared to bulk or solution systems. The continuous water phase will dissipate the heat of reaction and produce a polymer dispersion which can easily be processed due to its low viscosity environment. Clearly distinct from macroemulsion polymerization is

the absence of complex particle formation and mass transfer events and in this respect every miniemulsion droplet can be considered the clichéd nanoscale bulk reactor, completely segregated from the other droplets. This bulk environment has been shown to be suitable for living radical polymerizations in previous chapters.

The literature reports several attempts to perform living radical polymerization in miniemulsion, applying techniques based on reversible termination (ATRP, nitroxides).[19,20,21] The disadvantage of these approaches is the troublesome partitioning of the small deactivating species over the two phases, which complicates the kinetics[22]. If the deactivating species moves into the water phase it will slow the growth of aqueous phase radicals, interfering with the process of radical entry and thereby decreasing the rate of polymerization. Control of molar mass at the main locus of polymerization (*i.e.* inside the particle) will suffer from the reduced concentration of deactivating species. Besides, it has been argued that the persistent radical effect, which adds to the control in bulk and solution polymerizations, will cause an exceedingly low polymerization rate in such compartmentalized systems[23]. Although living radical polymerizations were conducted, the theory was confirmed in that the molar mass distribution was broader than polymerizations in a homogeneous medium.[21]

Techniques based on degenerative transfer form a more likely candidate for this type of application since, in theory, the number of free propagating radicals remains unaffected. Another advantage is that the controlling species is (attached to) a dormant polymer chain and thus will not be able to diffuse out of the particle, negating the effect of exit and the corresponding lack of molar mass control. Several studies reported the successful application of such techniques in waterborne systems, but most of these studies use relatively inactive species to control the polymerization. The alkyl iodides used by several groups[23,24,25] have a transfer constant only slightly larger than unity. A similarly slow consumption of the compound can be expected for the RAFT agents applied by Kanagasabapathy *et al.*[26,27] and in our own group,[28] because of a poor homolytic leaving group and a rather unactivated carbon–sulfur double bond, respectively. Although these systems allow the preparation of complex architectures (*e.g.* block copolymers[25]), polydispersity is usually high (~2) since the conversion of transfer agent into polymer chains takes place during a prolonged interval of the polymerization and because the exchange reaction between growing radicals and dormant chains is slow in comparison with propagation.

The transition from transfer agents with low activity to those with a high activity appears to be straightforward, but in practice this turns out to be more complicated. The previous chapter discussed the application of several RAFT agents in conventional emulsion polymerizations, both seeded[29] and *ab initio*.[30] In contrast to low activity xanthates which could easily be used,[28] high reactivity agents based on the dithiobenzoate group invariably led to colloidal stability problems.[29,30] A large amount of the transfer agent was lost in the form of (oligomeric) coagulum resulting in a much higher molar mass than was to be expected for the emulsion material. The application of high reactivity agents in miniemulsions is only preceded by two examples in the first patent detailing the RAFT process[31] and this will be the starting point of the investigations in this chapter.

Special care should be taken in approaching the 'ideal' situation described in the previous section (6.1.3) as any aberration from 100% droplet nucleation will push the system in the direction of the mechanisms and kinetics that prevail in macroemulsion polymerization.

If, on the one hand, only a small part of the original population of droplets is nucleated, the remainder will eventually act as monomer reservoir. The RAFT agent contained within these reservoirs should then be transported to the reacting particles through the water phase. This may have two different, but both undesirable effects. First, the RAFT agent arriving later at the locus of polymerization, will start new chains later in the polymerization, and therefore broaden the molar mass distribution. Second, if the RAFT agent has already been converted into (oligomeric) dormant species in these droplets, transportation may no longer be possible because of their low water solubility. The most probable event is that these oligomers eventually precipitate as monomer is depleted from these droplets.

If on the other hand secondary nucleation takes place, particles will be created that do not contain any RAFT agent as the transfer active moiety is attached to polymer chains in the first generation of droplets/particles. For this reason, the polymerization in these particles will not be controlled.

6.2. Anionic Surfactants

The combination of SDS and either hexadecanol or hexadecane as the costabilizer is beyond any doubt the most commonly applied stabilizer system for miniemulsion polymerizations. The first patent on RAFT polymerization[31] mentions two

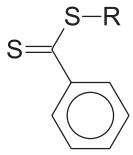

1. R = $C(CH_3)_2CN$
2. R = $C(CH_3)_2C_6H_5$
3. R = $C(CH_3)_2COOC_2H_5$
4. R = $C(CH_3)(CN)CH_2CH_2COO$-
-poly(ethylene-*co*-butylene)
5. R = poly(methyl methacrylate)

Scheme 6.2. RAFT agents applied in miniemulsion polymerizations. Their syntheses have been described in chapter 2.

examples of styrene miniemulsions using these components, and a similar system was taken as the starting point for our investigations. A series of preliminary experiments was conducted and this resulted in a remarkable observation.

Styrene miniemulsions, prepared using SDS as surfactant and hexadecane (with or without polystyrene) as the costabilizer, gave in most cases a visually stable miniemulsion. Miniemulsions are considered visually stable if they appear homogeneous to the eye, *i.e.* no separate organic or aqeous phase exists beside the emulsion phase. The droplet size was typically between 60 and 100 nm as measured by light scattering. When these miniemulsions were initiated with potassium persulfate (KPS), phase separation became apparent at the start of the reaction. A clear red monomer phase formed in the vortex of the stirred miniemulsion, and as the reaction proceeded this organic phase slowly increased in volume. The red color indicates the presence of species containing the dithiobenzoate group and GPC analyses revealed that the layer consisted of monomer swollen oligomers/polymers, usually of a considerably lower molar mass than the emulsion polymer and with a broader molar mass distribution (polydispersity typically between 3 to 5). This behavior is observed in all RAFT polymerizations stabilized with SDS, irrespective of the fact that in a variety of experiments the polymerization taking place in the emulsion phase below the organic layer exhibited living characteristics, *i.e.* a linear dependency of the number average molar mass on conversion.

Table 6.1: Overview of anionically stabilized miniemulsions[a)]

stabilization type	anionic
surfactant	SDS
monomer	styrene, BMA, EHMA
costabilizer	hexadecane, PS, Kraton
initiator	KPS, KPS/$Na_2S_2O_5$, AIBN, V-40, AIBN/V40
RAFT agent	**1**,**2**,**3**

a) These recipes typically apply 80 g water; 20 g monomer; 0.2 g surfactant; 0.2–0.5 g costabilizer; 0.2–0.6 g RAFT agent (2–4 g for **4** and **5**) and 0.1–0.2 g initiator.

Table 6.2: Anionically stabilized miniemulsions. Recipe details.

Experiment	AI-1	AI-2	AI-3	AI-4	AI-5	AI-6	AI-7
Monomer[a)] (g)	19.65	20.40	19.60	19.60	19.50	20.00[a)]	20.00[a)]
RAFT agent[b)] (g)	–	0.19	0.18	0.19	0.18	0.50	0.50
Water (g)	80.0	83.0	90.0	90.0	80.0	80.0	80.0
KPS (g)	0.12	0.11	0.14	0.25	0.14	0.20	0.20
SDS (g)	0.23	0.24	0.23	0.23	0.23	0.25	0.25
Hexadecane (g)	0.40	0.41	0.40	0.40	0.78	0.40	0.40
Fremy's Salt (g)	–	–	–	–	0.054	–	–
Sodium Bisulfite (g)	–	–	0.13	0.22	0.19	–	–

a) monomer is styrene except in AI-6 (EHMA) and AI-7 (BMA).
b) RAFT agent **2** was used.

Table 6.1 and Scheme 6.2 summarize the various monomers, RAFT agents and costabilizers that were used in combination with SDS in order to investigate this peculiar polymerization behavior.

6.2.1. Kinetics

To establish a basis for comparison of the accumulated data from RAFT experiments, a conventional styrene miniemulsion was performed in the absence of RAFT (AI-1). The recipe consisted of a typical miniemulsion concentration of SDS surfactant (0.01 mol·dm^{-3} H_2O) and a somewhat low concentration of KPS initiator (0.005 mol·dm^{-3} H_2O). This initiator concentration was chosen such that, when RAFT was added, transfer to RAFT agent or dormant RAFT polymer chains would dominate over bimolecular termination.[32] Table 6.1 provides a global overview of the ingredients used in the anionically stabilized miniemulsions while table 6.2 shows a more detailed description of the first series of miniemulsion polymerizations. A sample taken from AI-1 prior to initiation was monitored on shelf for several weeks with no visible monomer cream line, indicating a stable miniemulsion recipe. The miniemulsion recipe was then expanded to include RAFT agent **2** (see Scheme 6.2), with all other concentrations held constant (AI-2). In this manner, the effect of this RAFT agent on an otherwise stable system could be studied.

The conversion–time plots for the styrene polymerizations with and without **2** are given in Figure 6.1. A large drop in reaction rate is evident when comparing AI-1, (□, blank) to AI-2 (■, same recipe including **2**). In principle the nucleation of

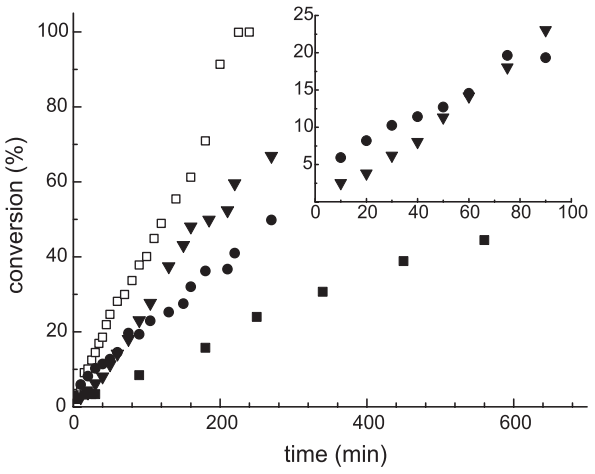

Figure 6.1. Conversion–time plots for miniemulsion polymerizations of styrene carried out at 75 °C, initiated by KPS. AI-1 (□), 'blank'. AI-2 (■), w/ RAFT. AI-3 (●), w/ RAFT & redox. AI-4 (▼), w/ RAFT & double redox.

the particles should be the same with and without RAFT agent. The decrease in rate can be attributed to two factors: ① exit of the transfer derived radical R (see Scheme 6.2) to terminate with radicals in the aqueous phase or termination by re-entry into a particle already containing a growing chain,[33,34] or ② termination of the entering propagating radical with the intermediate radical.[35] Based on the partitioning of radical R between the monomer and water phase, the large size of the droplets and the rate coefficient for re-initiation of radical R to monomer, the probability of exit is very low.[34,36] To further support this, the RAFT agent will be consumed within the first few percent of conversion (since $C_T \approx 6000$)[37]. Once the RAFT is consumed exit becomes even less probable due to the hydrophobicity and the low diffusion coefficient of the oligomeric chain, and should no longer affect the reaction rate. This suggests that retardation when **2** is added to the miniemulsion is due to termination of the intermediate radical, which has been shown to be the most likely mechanism at play in retarding the rate in bulk and solution experiments (page 43).[35]

A long polymerization time is not suprising, considering the relatively low propagation rate constant (k_p) for styrene[38] at 75 °C ($563\,dm^{-3}\cdot mol^{-1}\cdot s^{-1}$), the low entry rate (ρ) of persulfate initiated chains in styrene macroemulsions[4] and the low initiator concentration. However, when this slow rate is exacerbated by the retardation mechanisms described above, KPS decomposition becomes an issue at relatively low conversions. This is seen more clearly in Figure 6.2 where the experimental molar mass of polymerization AI-2 (styrene/RAFT) is compared to theoretical calculations. The solid points are the experimental values for the

number-average molar mass ($\overline{M}_n$) corresponding to the appropriate monomer conversion. The solid line represents the theoretical molar mass as calculated using Eq. 6-4,

$$\overline{M}_{n,\,th} = FW_{RAFT} + \frac{x \cdot [M]_0 \cdot FW_M}{[RAFT]_0} \qquad \textbf{(6-4)}$$

in which FW_{RAFT} is the molar mass of the RAFT agent that constitutes the end groups of the polymer chain; FW_M is the molar mass of a single monomer unit; x equals the fractional conversion, $[M]_0$ and $[RAFT]_0$ are the initial concentrations of the monomer and the RAFT agent in the droplets. Eq. 6-4 only accounts for RAFT-derived chain growth and neglects any products from radical–radical termination.

The dashed curve in Figure 6.2, calculated with Eq. 6-5, also represents a theoretical molar mass but additionally accounts for termination products. Their contribution can be quantified by the amount of initiator decomposed over the reaction time corrected by two efficiency factors and assuming termination by combination. $[I]_0$ is the initial concentration of initiator.[39] f_I is the initiator efficiency for addition of initiator radicals to monomer and f_{entry} is the efficiency of entry, *i.e.* the probability for a chain to enter a particle before aqueous phase termination occurs. Furthermore Eq. 6.5 requires k_d, the decomposition rate coefficient for initiator in the aqueous phase, $[M]_w$ the monomer concentration in the aqueous phase,[39] $k_{t,\,aq}$ the termination rate coefficient in the aqueous phase, z is the lowest number of monomer units required for the oligomer to be surface active, t is time in seconds and $[I]_w$ the initial concentration of initiator in the aqueous phase.[39]

$$\overline{M}_{n,\,theory} = FW_{raft} + \frac{x \cdot [M]_0 \cdot FW_M}{[RAFT]_0 + 2 \cdot f_I \cdot f_{entry} \cdot [I]_0 \cdot (1 - e^{-k_d t})} \qquad \textbf{(6-5)}$$

$$\text{with:} \qquad f_{entry} = \left(\frac{\sqrt{k_d \cdot [I]_w \cdot k_{t,\,aq}}}{k_{p,\,aq} \cdot [M]_w} \right)^{1-z}$$

Note that both Eq. 6-4 and Eq. 6-5 assume rapid and complete conversion of the RAFT agent into dormant species, a condition that, under normal circumstances, will be obeyed after a few percents of monomer conversion for the RAFT agents applied in this study.

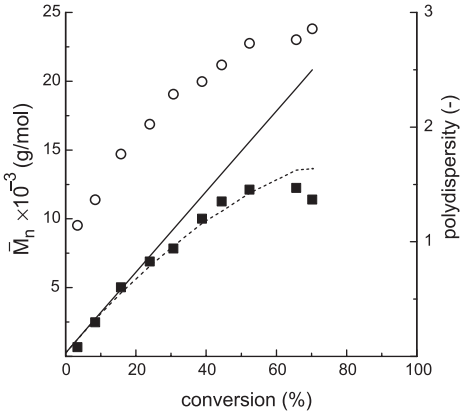

Figure 6.2. Number-average molar mass for miniemulsion polymerizations of styrene carried out at 75°C in the presence of SDS and RAFT, initiated by KPS (AI-2). Experimental $\bar{M}_n$ (■, *left axis*), Theoretical $\bar{M}_n$ accounting only for RAFT derived chains (—, *left axis*), Theoretical $\bar{M}_n$ accounting for RAFT derived chains and initiator derived chains (---, *left axis*). Polydispersity index (○, *right axis*)

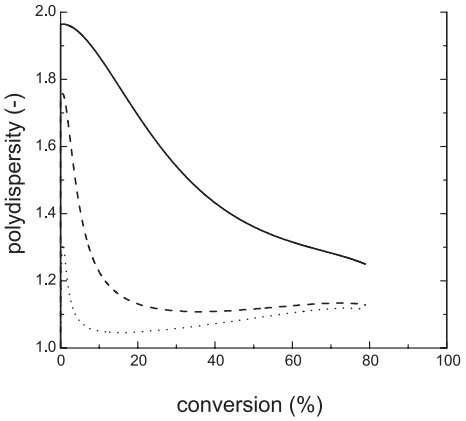

Figure 6.3. Simulations of the polydispersity index using Müller's equation.[40] Transfer constant (C_T) equals $6 \cdot 10^3$ (—), $6 \cdot 10^4$ (---) and $6 \cdot 10^6$ (·····).

Under most circumstances the second term of the denominator in Eq. 6.5 can be neglected relative to the concentration of RAFT agent since typical recipes apply a small amount of initiator compared to RAFT agent. The ratio of these two ingredients governs the amount of dead material as indicated by formula 6-6:

$$n_L = 1 - n_D = \frac{[RAFT]_0}{[RAFT]_0 + 2 \cdot f_I \cdot f_{entry} \cdot [I]_0 \cdot (1 - e^{-k_d t})} \qquad \textbf{(6-6)}$$

where n_L and n_D are the number fractions of living material and dead material, respectively. Terminated material not only excludes itself from further polymerization procedures (*e.g.* block copolymer preparation) but it also causes a broadening of the molar mass distribution. When the polymer molar mass and the maximum acceptable level of dead material are set, Eq. 6-5 and Eq. 6-6 give the ratio of monomer, RAFT agent and initiator. In solution and bulk polymerizations when a relatively pure or high molar mass material is desired this often leads to extremely low polymerization rates. With respect to the rate of polymerization, the situation is expected to be more favorable in dispersed systems where termination is reduced due to radical compartmentalization.

There are several points to be attention to with respect to Figure 6.2. Until roughly 25% monomer conversion, the theoretically derived molar mass relationship described by Eq. 6-4 is in good agreement with the experimentally observed molar mass. The linear relationship of $\overline{M}_n$ with conversion, matching theory, indicates living polymerization behavior. From roughly 25% conversion onward the experimentally determined $\overline{M}_n$ falls below the solid theoretically derived curve from Eq. 6-4. The data are now better approximated, however, by taking into account the presence of initiator-derived chains as described in Eq. 6-5. Due to the drastic retardation there is little conversion of monomer to polymer after approximately 70% but there is still an increase in the number of chains from initiator decomposition, thus the number average molar mass decreases.

More significant to note is the trend in the polydispersity index (○, *right axis*) which increased with conversion and reaction time. Figure 6.2 demonstrates that the polydispersity increases from a value of 1.1 (4% monomer conversion) to a final recorded value of 2.9 at 70% conversion. Theoretically,[40] in RAFT living systems, polydispersity should decrease with conversion ending close to unity upon full conversion if termination is negligible, *i.e.* if the number of initiator derived chains is small compared to the number of dormant chains. Using the method of moments derived by Müller *et al.*,[40] the theoretical profile of polydispersity is calculated in Figure 6.3 for the conditions of this run. The simulated polydispersity show that the system should in fact exhibit a decrease in polydispersity after the consumption of the RAFT agent. Also depicted in Figure 6.3 is the effect of the rate of consumption of the RAFT agent on the polydispersity. When C_T ($= k_{tr}/k_p$) is increased, the RAFT agent is consumed faster and the polydispersity is maintained at a lower value. The significance of this figure is that, in theory, the polydispersity of this system should be decreasing, in contrast to what is observed experimentally. The results given in Figures 6.2 and 6.3 reveal that initiation is a factor that cannot be ignored, and that it has a significant effect on the polydispersity.

A further observation from this data set that is not seen numerically, but that most definitely plays a role in the trends seen in Figure 6.2, is a distinct visual indication of an unstable miniemulsion, which has also been observed in macroemulsions[29,30] and in the preliminary experiments (page 144). The red organic phase slowly increases in volume making accurate sampling of the conversion impossible at longer reaction times. This stability issue will be discussed in more detail in section 6.2.2 and is stated at this point for the reader to better understand the phenomena that lead to the results presented in Figure 6.2.

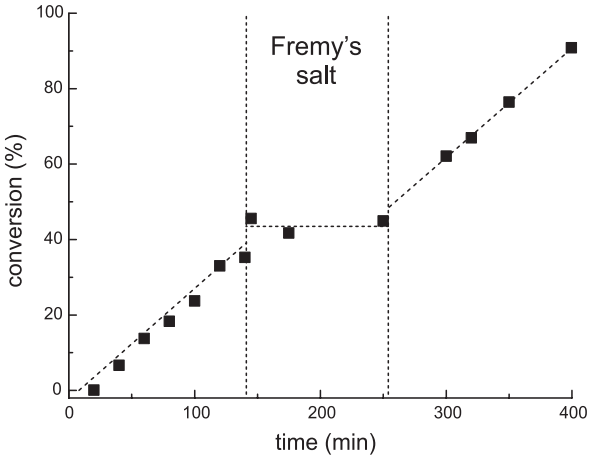

Figure 6.4. Conversion–time plot for AI-5 (■); miniemulsion polymerization of styrene using a redox system in the presence RAFT. Fremy's Salt was added at 45% conversion. (Note: the dotted line is a trend line, not a fit.)

The results from AI-2 suggest inefficient nucleation of the initial monomer droplet distribution due to the drastic retardation and the appearance of a red layer. To determine whether the red layer is caused by the low rate of polymerization a redox couple was added. Since a catalytic redox agent was not desired, but instead one that would merely aid in faster decomposition of KPS, sodium metabisulfite was chosen as the couple (AI-3). Its expediting action is confirmed by the addition of Fremy's Salt (potassium nitrosodisulfonate) at roughly 40% monomer conversion (AI-5, Figure 6.4). Potassium nitrosodisulfonate is a stable nitroxide radical that partitions strongly in the aqueous phase and will scavenge any carbon-centred radicals. It is modurately soluble in the droplets, so it may also terminate active chains in the particles. In Figure 6.4, monomer conversion is shown with the region of Fremy's Salt addition through to its consumption indicated. The Fremy's Salt did in fact stop the polymerization for roughly 100 min, *i.e.* the point at which it was fully consumed, after which polymerization continued at a similar rate to that prior to addition of Fremy's salt. This confirmed that the redox system is indeed an accelerator for initiator decomposition, and also allowed an approximate k_d value for the decomposition of initiator to be calculated, which is a required input parameter for the approximation of the number average molar mass by Eq. 6-5.

For the first 10% of monomer conversion (referring again to Figure 6.1), AI-3 (●, with RAFT and redox) showed no significant decrease in rate compared to AI-1 (□, no RAFT, no redox) of the same recipe and conditions. From 10% conversion onward, the rate of AI-3 (●, with RAFT and redox) was found to be less than that of the AI-1 (□, no RAFT, no redox), yet still markedly higher than that of AI-2 (■, RAFT system without redox). Assuming the same number of droplets initially

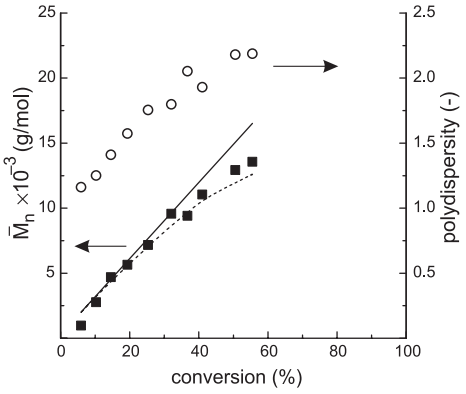

Figure 6.5. Number-average molar mass for miniemulsion polymerizations of styrene carried out at 75°C in the presence of SDS, RAFT agent **2** initiated by a redox couple (AI-3). Experimental $\bar{M}_n$ (■, *left axis*). Theoretical $\bar{M}_n$ accounting for RAFT derived chains only (—, *left axis*). Theoretical $\bar{M}_n$ accounting for RAFT derived chains and initiator derived chains (---, *left axis*). Polydispersity (○, *right axis*)

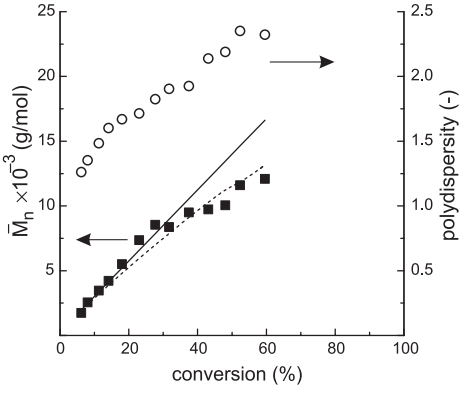

Figure 6.6. Number-average molar mass for miniemulsion polymerizations of styrene carried out at 75°C in the presence of SDS, RAFT agent **2** initiated by a redox couple (AI-4, [KPS] doubled from Figure 5). Experimental $\bar{M}_n$ (■, *left axis*). Theoretical $\bar{M}_n$ accounting for RAFT derived chains only (—, *left axis*). Theoretical $\bar{M}_n$ accounting for RAFT derived chains and initiator derived chains (---, l*eft axis*). Polydispersity (○, *right axis*)

present for both reactions, this indicated that a larger percentage of the initial droplet populatio was nucleated, effectively increasing the reaction rate. Figure 6.5 illustrates several beneficial effects of the redox agent on the evolution of the molar mass and polydispersity. Similar to the case without redox, the experimental molar mass agrees with the theoretically derived relations, yet with an increased reaction rate the disparity between the curve derived from Eq. 6-5 and the line described by Eq. 6-4 is less pronounced. Molar mass again showed contributions from initiator-derived chains and the polydispersity still has an upward trend. However, the polydispersity with redox initiation increased more slowly than that seen in Figure 6.2 (no redox, AI-1) and when it is compared at a monomer conversion of roughly 50% (2.18 in Figure 6.2 and 2.73 in Figure 6.5), the benefit of a greater number of droplets being nucleated is evident.

When the radical flux of the redox system was increased (by doubling both the concentrations of KPS and sodium metabisulfite), a further increase in polymerization rate was observed (AI-4, ▼, Figure 6.1). In fact, after the first 10% of conversion, the polymerization rate was comparable to that of the control experiment (AI-1). When the two redox systems are compared (inset, Figure 6.1) this becomes even clearer. The rate of the low radical flux recipe (AI-3, (●) is considerably higer

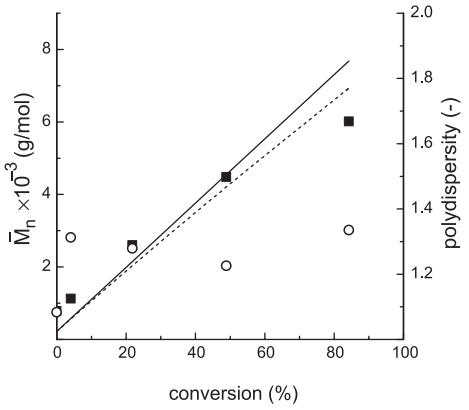

Figure 6.7. Number-average molar mass for mini-emulsion polymerizations of EHMA carried out at 75 °C in the presence of SDS, RAFT agent **1** initiated by KPS (experiment AI-6). Experimental $\bar{M}_n$ (■, *left axis*). Theoretical $\bar{M}_n$ accounting for RAFT derived chains only (—, *left axis*). Theoretical $\bar{M}_n$ accounting for RAFT derived chains and initiator derived chains (---, *left axis*). Polydispersity (○, *right axis*)

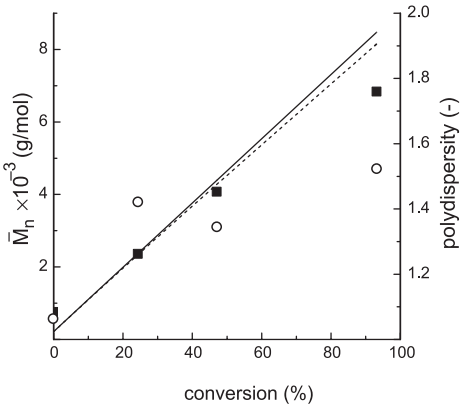

Figure 6.8. Number-average molar mass for mini-emulsion polymerizations of BMA carried out at 75 °C in the presence of SDS, RAFT agent **1** initiated by KPS (experiment AI-7). Experimental $\bar{M}_n$ (■, *left axis*). Theoretical $\bar{M}_n$ accounting for RAFT derived chains only (—, *left axis*). Theoretical $\bar{M}_n$ accounting for RAFT derived chains and initiator derived chains (---, *left axis*). Polydispersity (○, *right axis*)

than that of the recipe with the higher radical flux (AI-4, ▼) up to a conversion of roughly 14%, where the two profiles cross. The most probable explanation for the slower start of the higher radical flux run is a larger probability of termination in the aqueous phase, after which the rate is higher presumably due to a larger number of droplets nucleated. Conversion measurements after long reaction times in the redox reactions are not shown in Figure 6.1 as the formation of coagulum prevented accurate sampling.

A decrease of the ratio of [RAFT]/[KPS] will increase the amount of chains terminated by radical–radical reactions, and consequently produce a broader molar mass distribution as dictated by Eq. 6-6. This does not seem to be the case when the trends shown in Figure 6.6 are compared to those of Figure 6.5. The increase in radical flux of the system does not seem to have markedly affected the $\bar{M}_n$ or polydispersity. This is not unexpected since by increasing the number of particles, through a more efficient nucleation process, the entry rate (ρ) decreases and so does the amount of radical–radical termination[4].

In order to determine if the loss of colloidal stability is specific to styrene polymerizations, two experiments (AI-6 & AI-7) were performed keeping all other recipe concentrations constant while substituting methacrylic monomers for styrene

and substituting RAFT agent **1** for **2**. Methacrylates have higher propagation rate constants than styrene at 70 °C ($k_{p,styrene}$ = 440, $k_{p,BMA}$ = 1220 and $k_{p,EHMA}$ = 1470 $dm^{-3} \cdot mol^{-1} \cdot s^{-1}$).[41] The results indicated that macromolecular control with the methacrylates was much more easily achieved. Figure 6.7 and 6.8 both show the polydispersity to remain below 1.5, a dramatically lower value than that found in any of the styrenic systems, but regardless of better control the same miniemulsion destabilization phenomena were observed. With the higher reaction rate, the appearance of the red organic layer was much more immediate and up to 35 % of the organic material was lost to coagulation. This illustrates that the destabilization of the droplets is not related to the monomer type and seems to correlate to the reaction rate.

The next section attempts to investigate this behavior in anionically stabilized miniemulsions more thoroughly, while the use of other surfactants is discussed later in this chapter (starting on page 159).

6.2.2. Conductivity & pH Considerations

In an ideal stable miniemulsion, there should be no change in aqueous phase conductivity since there is negligible change in interfacial area, and consequently little rearrangement of surfactant[43,44]. Conversely, in a conventional (macro)emulsion the larger monomer droplets serve as reservoirs continually diffusing monomer across the continuous phase to the locus of polymerization in nucleated micelles. As these reservoirs are depleted, the total interfacial area in the system decreases and surfactant desorbs from the particle interface resulting in an increase in conductivity[44]. This is the theoretical foundation behind the conductivity experiments. Since a stable miniemulsion should exhibit a flat conductivity profile over conversion (all other factors constant, such as pH), an increase would indicate SDS being expelled from the particles into the aqueous phase. This may be the cause of the destabilization phenomena observed in the anionically stabilized systems.

Section 6.1.2 (page 136) made clear that the preparation of a miniemulsion typically leaves nothing more than a low equilibrium concentration (below the critical micelle concentration) of surfactant in the water phase and put the droplets in a critically stabilized situation. Coalescence slowly leads to a colloidally more stable situation without releasing surfactant to the continuous phase. With the

Table 6.3: Anionically stabilized miniemulsions. Recipe details.

Experiment	AI-8	AI-9	AI-10	AI-11	AI-12	AI-13	AI-14
Monomer[a)] (g)	14.83	14.83	14.83	14.83	22.26	14.66	14.66
RAFT agent (g)	–	–	0.14	0.14	0.21	0.14	1.37
Water (g)	60.0	60.0	60.0	60.0	90.0	60.0	60.0
KPS (g)	–	–	–	–	0.26	0.16	0.16
SDS (g)	0.17	0.17	0.17	0.17	0.27	0.17	0.17
Hexadecane (g)	0.30	0.30	0.30	0.30	0.53	0.30	0.30

a) monomer is styrene except in AI-9, AI-11 and AI-14 (EHMA).

excessive phase separation occurring in these miniemulsions it would be interesting to see how the conductivity evolves as this may yield information on the fate and the whereabouts of the surfactant during this process.

The first series of conductivity experiments (Table 6.3) compared the stability of miniemulsions on shelf to those of the same recipes when polymerized. The shelf experiments are miniemulsions without initiator that are stirred and kept at ambient temperature. Samples were taken over typical reaction times with further samples taken up to a time of three days. The shelf samples are all seen as a cluster of flat lines in the lower portion of Figure 6.9. These shelf experiments included 'blank' runs and those in the presence of RAFT for both styrene (experiments AI-8 and AI-10) and (2-ethyl)hexyl methacrylate (EHMA, experiments AI-9 and AI-11). Styrene was chosen due to the most pronounced level of instability observed in its miniemulsion RAFT systems, and EHMA was chosen for comparison purposes to see if instability was in any part a function of monomer characteristics. The flat profiles of all these shelf experiments suggest that the interaction of RAFT with other reagents is not a significant issue until polymerization is started. However, even in shelf samples, a small degree of instability was observed in the slow formation of a monomer cream line. The styrene shelf sample that included RAFT (Figure 6.9, □), showed a slight increase in conductivity but only after a shelf time of over 500 minutes. It should be noted that these shelf experiments were not under agitation.

Reacted samples, however, showed clear signs of an increase in surfactant concentration in the aqueous phase during polymerization, as evident in their increasing conductivity profiles in Figure 6.9. The styrene/RAFT miniemulsion polymerization at a reaction temperature of 75°C (AI-13, +) showed a more

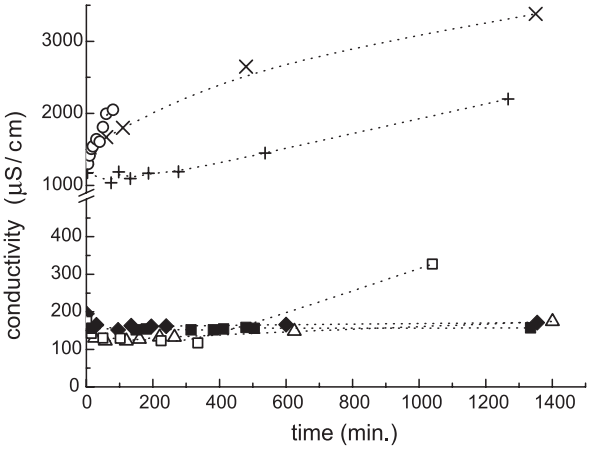

Figure 6.9. Conductivity of several styrene and EHMA miniemulsions 'on the shelf' (experiment AI-8, △; AI-9, ◆; AI-10, □; AI-11, ■) and during polymerization. (AI-12, ×; AI-13, +; AI-14, ○). See table 6.3 for experimental details.

dramatic increase in conductivity than that of the same reaction conducted at a reaction temperature of 45 °C (experiment AI-12, ×). The reaction involving EHMA and RAFT (experiment AI-14, ○) exhibited the fastest increasing conductivity. It seems that the conductivity increases in these reactions in a proportional manner to the rate of polymerization, similar to the correlation between the appearance of an organic phase and the polymerization rate.

The fact that the shelf experiments including RAFT did not show significant signs of increasing conductivity, while all reaction experiments did, leads to the conclusion that the destabilization is not only a matter of an incompatibility of the RAFT with typical emulsion components. Moreover, it suggests the key factor behind the observed destabilization has partially to do with oligomer formation which is the only distinction between the shelf and reaction experiments besides the temperature difference. The latter was found not to be important as tested by several verification experiments that were kept at higher temperatures.

An interesting point to note, however, is that when a styrene 'blank' polymerization (AI-8) was monitored for conductivity, the profile showed a downward trend over conversion eventually flattening out late in the reaction (not shown). This 'blank' was initiated by KPS, which is known to hydrolyze into sulfuric acid in an aqueous environment over time.[45] This effectively lowers the pH of the reaction medium with a profound effect on conductivity. In addition, the hydrolyzed form of KPS is no longer ionic – also affecting the conductivity towards lower values. For these reasons, sodium bicarbonate was added as a pH buffer and new reactions were again measured for conductivity, as shown in Table 6.4 and Figure 6.10.

Table 6.4: Anionically stabilized miniemulsions used for conductivity measurements.

Experiment	AI-15	AI-16	AI-17	AI-18	AI-19	AI-20	AI-21
Styrene (g)	21.91	14.12	17.11	20.00	19.80	19.65	19.35
RAFT agent (g)	–	0.13	0.16	–	0.20	0.35[a)]	0.65[a)]
Water (g)	90.0	60.0	70.0	80.0	80.0	80.0	80.0
Initiator[b)] (g)	0.24	0.16	0.56[b)]	–	–	–	–
SDS (g)	0.26	0.17	0.20	0.25	0.25	0.25	0.25
Hexadecane (g)	0.44	0.30	0.34	0.40	0.40	0.40	0.40
Sodium hydrogencarbonate (g)	0.09	0.06	0.07	–	–	–	–

a) These samples utilized an oligostyrene RAFT agent with degree of polymerization of 2 (AI-20) and 5 (AI-21).
b) Potassium persulfate is used as initiator except in AI-17, where AIBN was used.

In a buffered environment, after an initial increase in the first 25 minutes, the conductivity profile for the styrene 'blank' reaction (AI-15, □) in miniemulsion remained flat, as expected. The initial short lived rise in conductivity might be due to reactor contents coming to temperature. In a buffered environment the styrene RAFT miniemulsion polymerization, stabilized by SDS and initiated by KPS, showed no notable change in conductivity over the reaction timeframe (AI-16, ◆, Figure 10). Actually, the conductivity profile looked strikingly similar to the experiment without RAFT. This was a striking observation as the same recipe without buffer was found to be the most unstable. Even more significant is the appearance of the red organic phase in the vortex of the buffered styrene/RAFT miniemulsion polymerization although the conductivity was observed constant.

In attempt to rule out the sulfate group of the KPS initiator as a contributor to the RAFT destabilization phenomenon, a number of miniemulsion polymerizations were performed using 2,2'-azobisisobutyronitrile (AIBN) and 1,1'-azobis(1-cyclohexanecarbonitrile) (V-40) which are azo initiators that partition preferentially into the droplet phase. These miniemulsions differ from those initiated by KPS in several aspects. First of all, dissociation of these initiators does not change the pH. Second, the oligomers formed upon initiation are nonionic species so that there is no conflict between sulfate end-capped oligomers with the equally charged SDS surfactant. Third, oil phase initiation will suppress homogeneous nucleation if this would be present in the first place. Experiment AI-17 (●, Figure 6.10) is an example of such a polymerization. KPS was in fact proven not to be a large contrib-

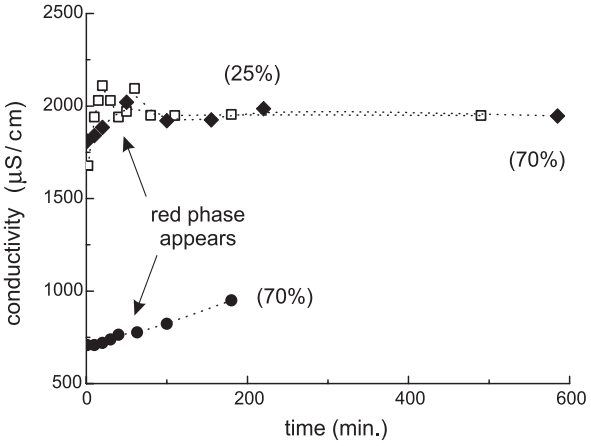

Figure 6.10. Conductivity of miniemulsion polymerizations of styrene under buffered conditions. 'blank' (AI-15, □), KPS w/ raft (AI-16, ◆), AIBN w/ raft (AI-17, ●). Conversion between brackets. See table 6.4 for experimental details.

utor (if at all) to the destabilization in these ionically stabilized systems. Even when initiated by AIBN, the same signs of destabilization and formation of the red organic layer were observed.

To achieve efficient nucleation of all particles, the radical flux was varied by changing the initiator from AIBN to V-40. While the stability remained poor it was found that the rate at which the organic layer was formed was (again) correlated to the speed of reaction; faster reactions exhibited faster formation of a separate organic phase.

It should also be noted here that the majority of radicals that partake in the polymerization are not derived from the initiator but originate from the applied RAFT agent. Its fast exchange reactions combined with its high concentration relative to that of the initiator causes the majority of both propagating and dormant species to have the R group, which was originally attached to the RAFT agent (Scheme 6.2), as end-group. Different RAFT agents (**1**, **2** and **3**) did not have any significant effect on the phase separation. Only when polymeric RAFT agents were used (**4** and **5**) some improvement could be observed. In these experiments the organic phase was much smaller in size and only slightly colored. The high weight fraction of polymeric species in the organic phase during the preparation of these miniemulsions disqualifies these experiments as suitable material to compare with the other polymerizations. This high weight fraction (up to 40%) is required to reach a comparable *molar* concentration of RAFT agent.

All the evidence presented points to the fact that phenomena occurring during the first few percents of conversion are the most pertinent to the destabilization of the miniemulsion. In this conversion period, small oligomers are created and exit into the aqueous phase is possible, thus forming the red organic layer. A distinct difference between these RAFT miniemulsion systems and traditional miniemulsion systems in the first few percent of monomer conversion is the chain length of polymer and the number of chains. In a traditional miniemulsion, much higher molar mass polymer would be formed when compared to that of a RAFT system at the same reaction time. If the particle interface were to undergo a great deal of traffic, as is the case with exit and re-entry of species at very low conversion, the presence of higher molar mass material would be expected to aid in the particle stability. However, when a small amount of polystyrene ($\overline{M}_w \approx 3\times10^5\,\mathrm{g\cdot mol^{-1}}$) is added to the organic phase no improvement in stability could be noted. The presence of oligomers therefore seems to be more disastrous than the lack of high molar mass material.

To test the conjecture that dormant oligomers are the key factors behind most of the discussed phenomena, the conductivity of miniemulsions in the presence of specially prepared oligomeric species was monitored in static experiments designed to mimic stages of a miniemulsion. Conditions of these runs were similar to the previously discussed shelf conductivity experiments, yet the contents were stirred under argon (without heating) and were monitored for over three weeks. The synthesized oligomers were prepared by solution polymerization from a reaction of 0.2 g of RAFT with styrene and AIBN. The isolated oligomers were dissolved in the usual organic medium of styrene and hexadecane while the amount of styrene was adjusted in such a way that the total mass of dormant species, RAFT and styrene was the same as would be in an actual polymerization. These miniemulsions however, were not polymerized, but the conductivity of these systems was monitored over time without reaction taking place. This data set consisted of a 'blank' (AI-18), a normal RAFT experiment (AI-19), a synthesized short dormant oligomer (AI-20, average of 2 monomer units), and a synthesized long dormant oligomer (AI-21, average of 5 to 6 monomer units).

Just from the conductivity data in Figure 6.11, it can be concluded that the RAFT agent does in fact play a role in destabilization and the longer it grows the smaller the effect. Apparently the length of oligo2 (the longer synthesized oligomer) is already such that the added stability through its contribution to the osmotic pressure is at least as large as its destabilization effect. That is, the oligo2

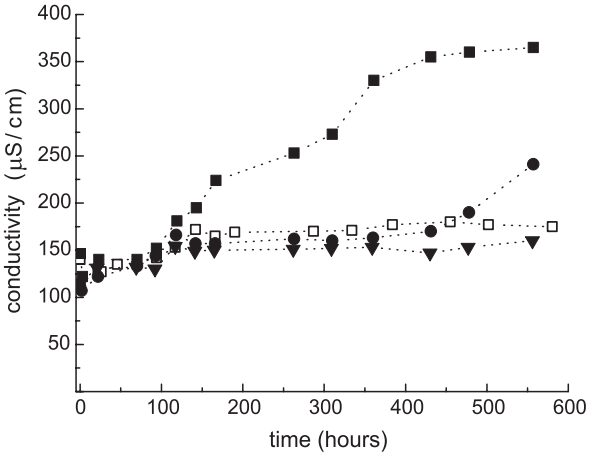

Figure 6.11. Conductivity of miniemulsion polymerizations of styrene carried out in the presence of different RAFT agents. AI-18 (□), no RAFT. AI-19 (■), raft. AI-20 (●), with short oligomers. AI-21 (▼), with longer oligomers. Experimental details are given in table 6.4

curve is remarkably similar to the 'blank' curve on Figure 6.11. However, conductivity does not divulge everything as the reactor contents showed clear signs of the red organic phase within a few hours while the conductivity of oligo1 (the short synthesized oligomer) does not show signs of instability until around 3 weeks after the inception of the experiment.

Possibly a more significant observation is that destabilization is observed at a maximum when RAFT miniemulsions are initiated. This destabilization effect is also observed much faster than seen in any of the 'static' experiments. This suggests that the destabilization is due to more than just the *presence* of oligomeric species because in the reaction experiments polymers grow to the 'stable' oligo2 chain length (roughly 5 monomer units) quite rapidly.

6.3. Cationic Surfactants

In an attempt to circumvent this stability issue, a different stabilization strategy was adopted from literature where it was shown that cetyl trimethyl ammonium bromide (CTAB), a cationic surfactant, could stabilize miniemulsions with an efficiency similar to that of SDS.[48] A series of miniemulsions was conducted employing this surfactant and 2,2'-azobis[2-methyl-N-(2-hydroxyethyl)propionamide] (VA-086) as initiator (Table 6.5). Again stable miniemulsions were obtained after sonication but phase separation was induced by the polymerization. Similar variations were made in the choice of hydrophobe and RAFT agent as in the series of SDS experiments, all with similar results in terms of stability. These systems typically react until the monomer is depleted from the 'emulsion phase'. In

Table 6.5: Cationically stabilized miniemulsions [a)]

stabilization type	cationic
surfactant	CTAB
monomer	styrene
costabilizer	hexadecane, PS, Kraton
initiator	VA-086, AIBN, V-40
RAFT agent	**2**,**3**,**4**,**5**

a) These recipes typically apply 80 g water; 20 g monomer; 0.2 g surfactant; 0.2–0.5 g costabilizer; 0.2–0.6 g RAFT agent (2–4 g for **4** and **5**) and 0.1–0.2 g initiator.

the end situation the organic layer would contain up to 40% of the total amount of monomer of which a substantial part had been polymerized. The emulsion material itself was of very low molar mass and had a multimodal distribution. In these experiments, polymeric RAFT agents (Scheme 6.2, agents **4** and **5**) were also investigated but these could not completely suppress the instability. Although the dithiobenzoate moiety was attached to a hydrophobic polymer chain, trapped in the droplet phase, a small organic phase with a light red color was formed.

6.4. Nonionic Surfactants

The third alternative way to stabilize miniemulsions comprises the use of nonionic surfactants. Recent literature reports the successful application of such surfactants in polymerizable miniemulsions.[48,49] A variety of nonionic surfactants was used in conjuction with hexadecane (alone or in combination with Kraton) as the hydrophobe. Application of surfactants with relatively high HLB values (15.3–17.8) in most cases led to stable miniemulsions. Samples taken from the unreacted emulsions were monitored for at least a week and during this period only a few cases showed some signs of creaming or destabilization after 4 to 5 days; the majority remained homogeneous to the eye. These miniemulsions typically reacted in the absence of an organic layer. Under some circumstances minor phase separation was observed 10 to 20 minutes after the start of polymerization, but quickly thereafter it would disappear without notable effect on the molar mass distribution and without the formation of any coagulum. The products from the polymerizations were stable for at least several months. The results of several such polymerizations are discussed in the sections ‘controlled polymerization’ (page 162) and ‘block copolymers’ (page 166).

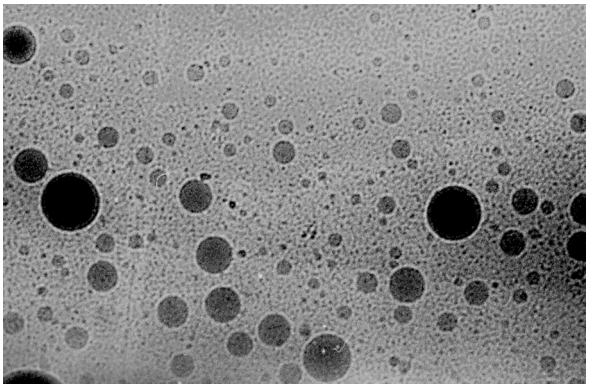

Figure 6.12. Cryo TEM image of a polymerized miniemulsion, stabilized by Igepal890, a nonionic surfactant (NI-2, see table 6.7). The number average particle size is 290nm, but the distribution is of high polydispersity, possibly caused by monomer migration in the early stages of the polymerization.

The reason why nonionic surfactants are able to provide enough stability where the ionic surfactants fail is not clear. The investigations with the miniemulsions using SDS were particularly in depth, but using alternative ingredients for each and every one of the miniemulsion components could not reveal the particular perpetrator. Moreover, Matyjaszewski *et al.*[20] report strikingly similar observations of instability in studies of ATRP polymerizations in dispersed media and El-Aasser *et al.*[19] report data that imply similar instability phenomena are occurring in nitroxide mediated living miniemulsion polymerization, which indicates that the cause should not be sought in the specific RAFT chemistry. The only literature that does not indicate instability phenomena is that of RAFT agents (of the xanthate type)[28] or degenerative transfer agents (e.g. perfluorohexyl iodide),[24] however, polydispersity stays relatively high (1.5–3.2).[30,46] The distinction between the alkyl iodide system and the RAFT agents of this chapter is the activity of the chain transfer agent ($C_{T,styrene}$=1 to 1.4 for $C_6F_{13}I$)[23,47] which dictates that the molar mass at low conversions is close to the final $\overline{M}_n$ when using a RAFT agent with a very high C_T[40]. This further emphasizes the role of oligomers in the destabilization phenomena seen in (mini)emulsion polymerization with highly active chain transfer agents. When different stages occurring in such a polymerization were simulated by predissolving oligomers in the organic phase (AI-18 to AI-21) the stability was affected on the long run but appeared much better than in an actual polymerization. The only difference between a polymerization and the static experiments with oligomers is the distribution of these species over the droplets. By predissolving them, they are equally divided among the miniemulsion droplets while in a reaction they are generated in large amounts in individual droplets, namely those that are struck by a radical. Due to the high reactivity of the RAFT agent, a single radical can transform a lot of transfer agent molecules into dormant oligomers with a much lower water solubility adding considerably to the osmotic pressure in that particular

Table 6.6: Experimental details homopolymerizations with nonionic surfactants[a)]

ingredient	quantity (g)	quantity (mmol)	type
water	80		
monomer	20	100–200	see table 6.7
surfactant	4.0	2.0	Igepal 890
co-stabilizer	0.40	1.8	hexadecane
initiator	0.20	0.75	KPS
RAFT agent[b)]	0.60	2.5	**1**

a) NI-1 to NI-6
b) no RAFT agent was present in the control experiment NI-1

droplet. Although it is not necessary for a miniemulsion to be in a thermodynamically stable state, an important factor for metastability is an equal chemical potential in all droplets. This condition may be quickly lost as the polymerization commences. Based on all the experimental results gathered in this chapter, the dynamic 'dropwise' generation of oligomers seems to be the most likely cause of the destabilization. Apparently the nonionic surfactants impose better stability on the droplets but the same forces are present in these systems. Support for this hypothesis can be found from the particle size distributions which are broad for miniemulsions with RAFT as can be seen in Figure 6.12.

6.5. Controlled Polymerization

6.5.1. Homopolymerizations & Kinetics

Once stability was guaranteed, miniemulsions could be used as a tool in the preparation of sophisticated polymer architectures. Tables 6.6 and 6.7 provide details on a series of miniemulsions that was conducted in the presence of a nonionic surfactant.

Figure 6.13 shows conversion–time profiles for several miniemulsion polymerizations. When the rate of the experiment without RAFT (NI-1, table 6.7) is compared with that of the same experiment with RAFT (NI-2) it is shown that the addition of RAFT agent to the system causes a large decrease in the rate of polymerization. The reaction rates for the various methacrylates are roughly proportional to their propagation rate constants which have the same order of magnitude. Only the methyl methacrylate (MMA) polymerization showed deviating behavior.

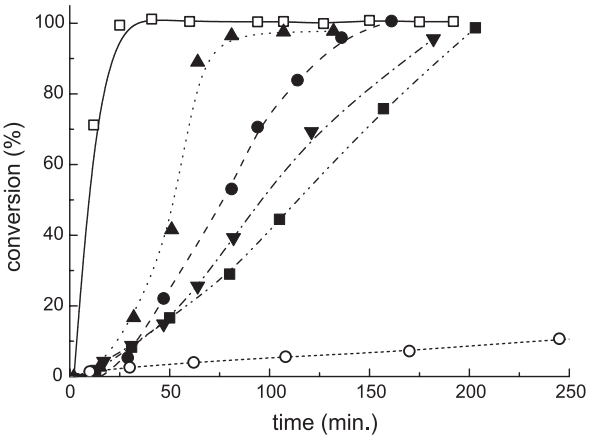

Figure 6.13. Conversion-time profiles for miniemulsion polymerizations: NI-1(□), NI-2(●), NI-3(▲), NI-4(▼), NI-5(■) and NI-6(○). See tables 6.6 and 6.7 for the experimental details of these polymerizations.

Due to its smaller particle size and consequently larger number of particles, it was expected to react faster. It initially, however, starts at a comparable polymerization rate but shows a notable acceleration during the first 40 minutes. It is unlikely that this can be attributed to the gel effect that is quite commonly observed in methyl methacrylate polymerization, since over this time interval the average polymer chain length does not exceed 30 repeat units. For a PMMA sample of such a chain length prepared in solution polymerization, the glass transition temperature (T_g) was found to be 85 °C, well below the literature value for high molar mass material of approximately 110 °C. As the droplets consist of only 20 % of this polymeric material dissolved in about 80 % of monomer at a reaction temperature of 70 °C, the gel effect is unlikely to occur. Another explanation is that additional particles are generated during this interval. The more hydrophilic MMA monomer and its oligomers may promote homogeneous nucleation and in this way increase the number of particles and thus the reaction rate. The newly formed particles would be deficient in RAFT agent resulting in uncontrolled polymerization. However, no evidence for such a process is found in the molar mass distributions.

The most likely explanation is the increased entry efficiency of MMA compared to *n*-BMA, *i*-BMA and EHMA. It has been calculated that the entry efficiency for MMA and BMA at 50 °C and at a KPS concentration of 0.01 mol·dm^{-3} were 94% and 15%, respectively,[4] and therefore MMA will have a higher average number of radicals per particle compared to BMA. The origin of this effect can be traced back to the greater water solubility of MMA.

Table 6.7: Experimental details for miniemulsions stabilized by nonionic surfactants

number	monomer	time (min.)	x (%)	$\overline{M}_{n,theory}$ ($\times 10^{-3}$ Da)	$\overline{M}_n$ [a)] ($\times 10^{-3}$ Da)	$\overline{M}_w/\overline{M}_n$ (–)	dp (nm)
NI-1	EHMA	25	100	–	>3000	–	–
NI-2	EHMA	29	5	–	–	–	–
		47	22	–	–	–	–
		81	53	4.1	5.4	1.07	–
		94	71	5.4	6.1	1.08	–
		114	84	6.4	6.7	1.08	–
		136	96	7.3	7.3	1.09	–
		161	100	7.6	7.6	1.09	290
NI-3	MMA	32	14	1.3	–	–	–
		51	38	3.2	5.3	1.07	–
		64	84	6.7	7.9	1.15	–
		81	95	7.4	8.3	1.17	160
NI-4	i-BMA	17	4	0.57	–	–	–
		31	9	0.90	2.0	1.10	–
		47	15	1.3	–	–	–
		64	26	2.1	4.9	1.07	–
		82	40	3.1	5.5	1.11	–
		121	70	5.3	6.8	1.19	–
		182	96	7.3	8.2	1.25	300
NI-5	n-BMA	31	8	0.93	–	–	–
		50	17	1.6	–	–	–
		80	29	2.6	4.9	1.06	–
		105	45	3.9	5.5	1.10	–
		157	76	6.5	7.0	1.17	–
		203	99	8.4	8.5	1.20	300
NI-6	STY	108	6	0.72	0.73	1.07	–
		170	7	0.86	0.78	1.06	–
		245	11	1.2	0.94	1.08	–
		348	14	1.4	1.3	1.13	–
		1280	42	4.0	4.3	1.12	221
NI-7	STY	66	5	8.0	8.0	1.12	–
		99	9	8.3	8.1	1.14	–
		180	16	8.8	8.4	1.17	–
		305	28	9.7	9.0	1.20	–
		2525	87	14	12	1.38	340
NI-8	MMA	32	41	9.3	9.1	1.23	–
		67	96	13	11	1.40	–
		140	100	13	11	1.40	240; 340
NI-9	EHMA	27	9	0.99	–	–	–
		42	29	2.6	3.5	1.09	–
		55	39	3.5	3.9	1.11	–
		67	56	4.8	4.6	1.13	–
		99	89	7.5	6.4	1.13	–
		125	99	8.4	7.1	1.10	–
	+ MMA/MA	165	–	–	7.9	1.11	–
		190	–	–	9.1	1.13	–
		215	–	–	1.0	1.16	230

a) Experimental molar masses are determined by GPC against polystyrene calibrants.

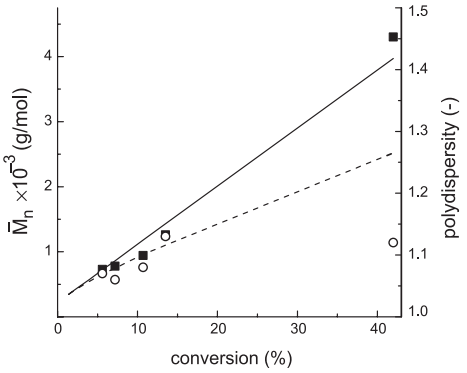

Figure 6.14. Results for the polymerization of styrene (NI-6). Number average molar mass: experimental values (■, in PS equivalents); theoretical values based on the dormant species (—); theoretical values corrected for initiator derived chains (---). Polydispersity index of the polymer (○, *right axis*).

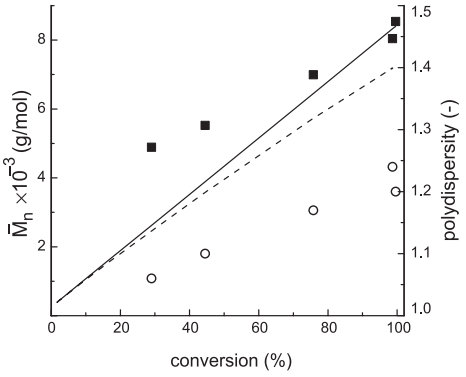

Figure 6.15. Results for the polymerization of *n*-BMA (NI-5). Number average molar mass: experimental values (■, in PS equivalents); theoretical values based on the dormant species (—); theoretical values corrected for initiator derived chains (---). Polydispersity index of the polymer (○, *right axis*).

The exceptionally low rate of the styrene polymerization can be explained by its lower propagation rate constant (k_p) combined with the fact that it has been shown to be stronger affected by the retardation inherent in RAFT polymerization.

Again Eq. 6-4 and Eq. 6-5 can be used to evaluate the evolution of the number-average molar mass with conversion and time. Figure 6.14 and Figure 6.15 show two predictions for molar mass. An overestimation is obtained when the initiator-derived chains are neglected (Eq. 6-4), denoted by the solid straight line. The dashed curve is an underestimation of the molar mass, and depicts the situation when $f_I \times f_{entry}$ equals 0.7, assuming that entry efficiency equals unity and initiator efficiency is 0.7 similar to solution experiments. As mentioned previously the difference between the two predictions often is negligible, but it becomes clear from Figure 6.14 that for slow polymerizations the time dependent term describing the initiator contribution plays a role. The styrene polymerization (Figure 6.14) closely follows the predicted values over the studied conversion range while the butyl methacrylate polymerization (Figure 6.15) seems to start above theory and slowly converges on the theoretical values. A reason for this behavior should not be sought in the miniemulsion kinetics as a similar trend was observed in solution polymerizations. The difference can be explained by the fact that the experimental molar mass has been determined by gel permeation chromatography (GPC) against polystyrene standards. Although Mark–Houwink parameters are available for the applied methacrylates such a correction procedure is known to yield unreliable

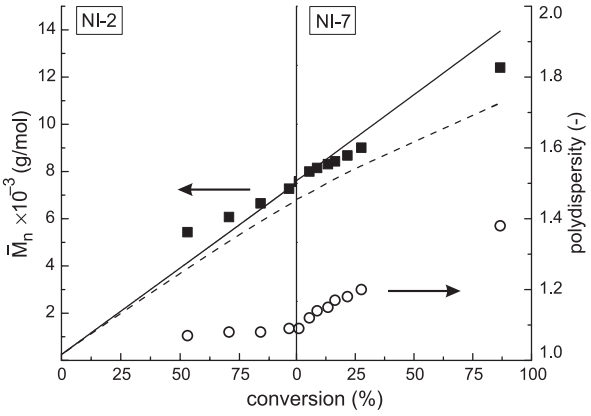

Figure 6.16. Molar mass data (*left axis*) for the preparation of the seed latex (NI-2) and the subsequent seeded polymerization of styrene (NI-7). Number average molar mass: experimental values (■, in PS equivalents); theoretical values based on the dormant species (—); theoretical values corrected for initiator derived chains (---). Polydispersity index of the polymer (○, *right axis*).

results for low molar mass polymer. The same drift is observed in the polymerization of EHMA, depicted on the left hand side of Figure 6.16. All of these polymerizations show living behavior with low polydispersities (<1.20).

6.5.2. Block copolymers

The living character of the miniemulsions was further instanced by their transformation into block copolymers. This was done either by two subsequent batch polymerizations where the initially prepared miniemulsion serves as a seed for the second polymerization or by a semi-continuous procedure where a second monomer was added to the polymerization reaction over a certain time interval, just after the first monomer had reached full conversion.

In the batch polymerizations the product of NI-2 was applied as the seed latex for experiments NI-7 and NI-8 (see Table 6.7, on page 164 for details). For each of these experiments the seed was swollen with an amount of monomer equal to the amount of polymer already present (on weight basis). A small amount of surfactant

Table 6.8: Block copolymers by batch reactions

ingredient	quantity (g)		
		7.0	PEHMA
latex NI-2	35	1.4	Igepal890
		0.04	KPS
monomer	7.0	STY (NI-7) / MMA (NI-8)	
surfactant	0.8	Igepal890	
initiator	0.04	KPS	

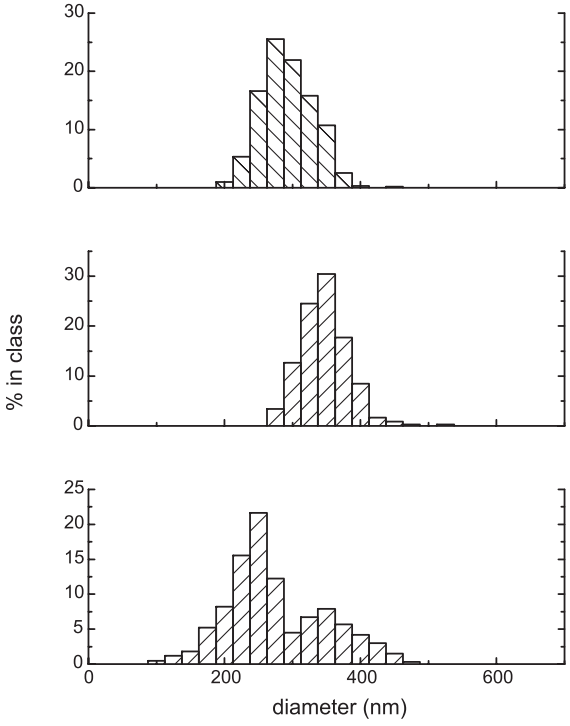

Figure 6.17. Particle size distributions for experiments NI-14 (*top*), NI-15 (*middle*) and NI-16 (*bottom*). In polymerization NI-15, the polymerization has taken place exclusively in the existing particles, therby enlarging them. In experiment NI-16, both the existing particles have grown while the material is transformed to diblock copolymer material while a new crop of particles is generated with a diameter of approx. 240nm. These patricles most likely consist of high molar mass PMMA homopolymer.

was added to stabilize the increased surface area of the particles. Assuming a constant number of particles, then doubling the volume will increase the total surface area with approximately 60%. The initiator concentration was brought back to the same level as at the start of the seed latex preparation NI-2. From the reaction time and the dissociation rate constant, KPS was assumed to be consumed for about 50%.

In polymerization NI-7, styrene is employed and due to its low k_p, the rate of polymerization is much lower than that of NI-2. Figure 6.16 shows the continued increase in molar mass of the seed latex material. Again the low polymerization rate suggests that Eq. 6-5 be implemented to account for chains started by initiator. The experimental values are between the theoretical line not taking into account initiator, and the curve using Eq. 6-5 with f equal to 0.7. Although the polydispersity increased during this second stage of the polymerization it remains low (1.38). The particle size (number-average) increased from 0.29µm for NI-2 to 0.34µm for NI-7. If a constant number of particles is assumed, then adding 87% to the volume of the particles (conversion of NI-7) should increase their diameter by approximately 23%, going up to 0.36µm. The difference between theory and measurement is small and no evidence for secondary particle formation could be found.

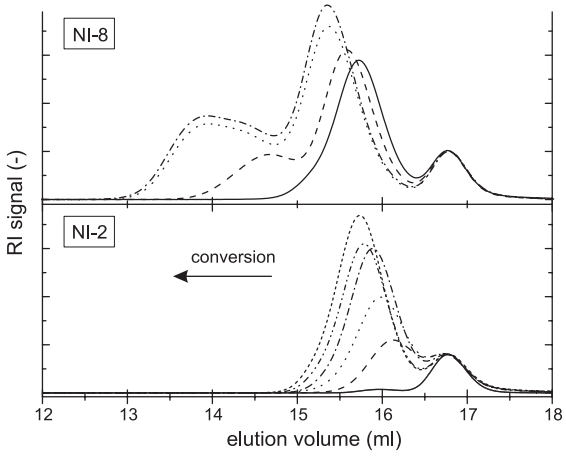

Figure 6.18. GPC traces (refractive index detector) for the preparation of the seed latex (NI-2, *bottom*) and the subsequent seeded polymerization of MMA (NI-8, *top*). The peak at 16.8 ml corresponds to the applied nonionic surfactant. This peak was used for normalization.

In polymerization NI-8, in which the seed latex is swollen with MMA, the reaction proceeds faster than the preparation of the seed (NI-2, same [KPS] and temperature), though the k_p of MMA is slightly lower than that of EHMA.[50] Again the high entry efficiency found for MMA polymerizations may play a role but a more important effect in this case is the generation of a new crop of particles. This process is confirmed by the particle size distribution as well as the evolution of the molar mass distribution. Doubling the volume of the original particles (MMA conversion is 100 %) would increase their diameter from 0.29 µm to 0.37 µm. The particle size distribution (Figure 6.17) shows that the original population has grown only to 0.34 µm and that new particles are generated with a particle size of 0.25 µm. The newly formed particles will not contain any dithioester groups as these are securely attached to polymer chains in the original population of particles. For this reason polymerization in these particles will proceed in an uncontrolled manner and high molar mass PMMA homopolymer will be formed. This is confirmed by the GPC traces depicted in Figure 6.18.

The signal at an elution volume of 16.8 ml THF corresponds to the nonionic surfactant and has been used for normalization purposes. During the polymerization of EHMA (NI-2), low polydispersity material is formed with a number-average molar mass of $7.6 \cdot 10^3 \, g \cdot mol^{-1}$ (PS equivalents). During the seeded polymerization (NI-8), this material continues growing as it is being converted into poly(EHMA-*b*-MMA) and retains its narrow distribution. Simultaneously, material of high molar mass and higher polydispersity is formed which we expect to be PMMA homopolymer in the second crop of particles. It grows in a conventional uncontrolled fashion

Table 6.9: Block copolymer by a semi-continuous procedure (NI-9)

		quantity		
	ingredient	(g)	(mmol)	type
batch	water	80		
	monomer	20	100	EHMA
	surfactant	4.0	2.0	Brij98
	costabilizer	0.40	1.8	hexadecane
	costabilizer	trace		Kraton
	initiator	0.20	0.75	KPS
	RAFT agent	0.60	2.5	1
feed stream[a)]	monomer	9.2	92	MMA
	monomer	0.8	9	Methacrylic Acid

a) The monomer feed stream was started at a rate of 0.1 ml/min. two hours after the start of the reaction. At this point, the polymerization of EHMA was complete.

due to the absence of dithioester species, confirmed by the absence of the dithiobenzoate chromophore in the chromatogram generated by the UV detector at a wavelength of 320nm (not shown).

Here we have prepared a latex, which may have very intriguing properties as it contains both high T_g particles of high molar mass and particles consisting of a low molar mass block copolymer that can act as *in situ* compatibilizer for the PMMA spheres and another material. Alternatively, the hard PMMA spheres may act as reinforcement filler for the block copolymer film cast from this latex. Indeed living radical polymerization in miniemulsion can open up the way to a whole new class of "designer-latices".

Experiment NI-9 differs from NI-2 in that it utilizes Brij98 as surfactant (table 6.9). In this polymerization block copolymer is prepared by a semi-batch procedure. First EHMA is polymerized to full conversion. The molar mass is again close to the theoretical value and polydispersity remained below 1.2 (Figure 6.19). A feed stream of a 10g monomer mixture of MMA and methacrylic acid (12:1 on weight basis) was started at a rate of $0.1\,ml \cdot min^{-1}$. Samples taken during this part of the polymerization again exhibit controlled growth of the block copolymer. The GPC traces showed no evidence of non-block copolymers formed during this stage – in this case poly(MMA-*co*-methacrylic acid). Non-block copolymers are unavoidably formed to some extent and although their amount can be minimized, they are usually observable as low molar mass material in the GPC trace when block copolymers are prepared in bulk or solution.[51] The combination of high polymerization

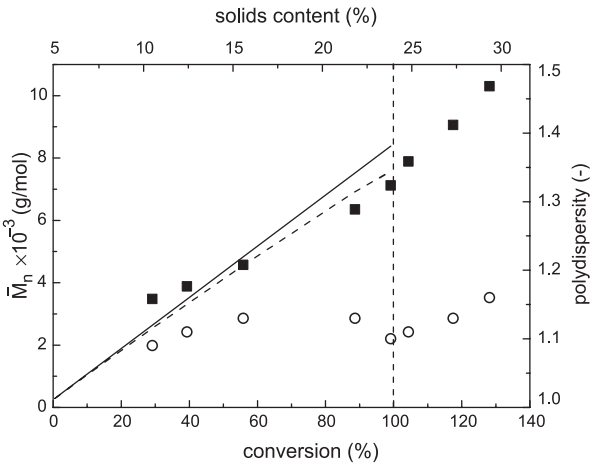

Figure 6.19. Molar mass data (*left axis*) for polymerization of EHMA (NI-9) and its transformation into poly(EHMA-*b*-[MMA-*co*-methacrylic acid]). Number average molar mass: experimental values (■, in PS equivalents); theoretical values based on the dormant species (—); theoretical values corrected for initiator derived chains (---). Polydispersity index of the polymer (○, *right axis*).

rate and low radical flux per particle – typical of compartmentalized systems – allows the preparation of block copolymers with a higher degree of purity than that is typically achieved in homogeneous media.

The high purity of block copolymers in compartmentalized systems is a function of the entry rate coefficient. This means that the polymerization rate can be increased by increasing the number of particles which in turn decreases the entry rate coefficient and thus improves the purity of the blocks produced.

To further establish the effectiveness of this procedure, the samples were precipitated in water/methanol (3:1) to remove the surfactant and analyzed by HPLC (Figure 6.20). Chromatograms were normalized on the Kraton (eluting around 3 min), a trace of which had been mixed in the organic phase as an internal standard. Several samples of different PEHMA chain lengths were injected and these gave two peaks between 6 and 8 min elution time. The three samples taken during the second stage of the polymerization (see table 6.7) had much higher elution volumes. The first has added an average number of only 7 monomer units per chain resulting in a very broad multimodal signal barely visible above the baseline between 9 and 32 ml elution volume. The exact elution volume is strongly dependent on the number of polar monomer units that has been added and especially on the incorporation of methacrylic acid. As the chains grow further and all start to contain methacrylic acid, the polymer elutes at 30 ml. The nonionic surfactant Brij98 eluted at 34 ml and was not present in the precipitated samples. Integration of the peaks revealed that less than 2% of the poly(EHMA) prepared in the first stage remained and the absence of its signal in the UV chromatogram (λ=320nm)

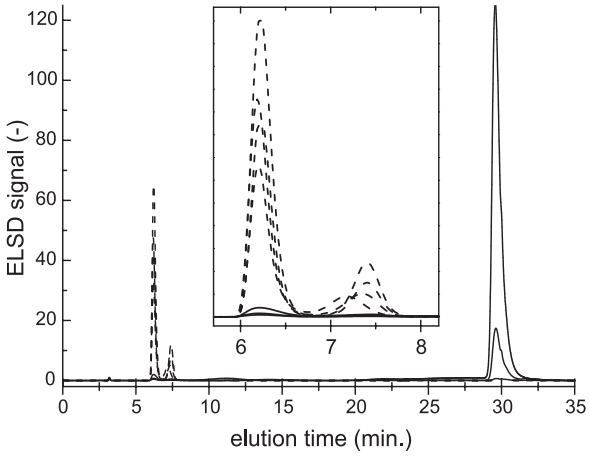

Figure 6.20. Gradient HPLC chromatograms of samples taken from miniemulsion NI-9. Samples taken during the polymerization of EHMA (---) and samples taken during the addition of the second monomer feed stream of MMA and methacrylic acid(—)

showed that these chains no longer have a dithiobenzoate end group. No peaks other than this one and the one attributed to the block copolymer were observed. This leads us to conclude that very narrow polydispersity poly(EHMA-*block*-[MMA-*co*-methacrylic acid]) was prepared with the surfactant as the single significant contaminant. The product was easily isolated by precipitation in water/methanol.

6.6. Conclusions

The application of RAFT polymerizations in dispersed media is not as simple as might be expected from its straightforward free-radical chemistry. After previously reported difficulties using *ab initio* and seeded emulsion polymerizations it was expected that elimination of the need of the RAFT agent to be transported through the water phase would alleviate the encountered stability problems. This was found not to be the case in miniemulsion polymerizations using RAFT. Both anionic and cationic surfactants were found inadequate in maintaining the original droplet morphology upon the onset of reaction. A separated organic phase would appear, combined with a polymer product of relatively high polydispersity. Variations on the ingredients of the recipe did not result in identification of any particular deleterious component, although it must be said that there is only limited understanding of the interaction of the RAFT agent with other emulsion components at this point.

Quite remarkably, similar phenomena are reported in ATRP and nitroxide mediated polymerization which support the hypothesis that the cause of the destabilization should not be sought in specific chemical interactions or reactions of the RAFT system as these techniques apply completely different components to control the polymerization. One characteristic feature that they have in common and which distinguishes them from a conventional uncontrolled miniemulsion polymerization, is the existence of a time interval early in the reaction where oligomeric species dominate the molar mass distribution of both the inactive chains and the propagating radicals. Beyond any doubt, this will have a tremendous influence on kinetic issues like radical desorption, termination, and droplet nucleation.

The destabilization could not be simulated, however, by the deliberate addition of oligomers to the organic phase prior to the emulsification, which indicates that the dynamic formation of oligomers in the course of reaction is an important aspect. In this process droplets are generated with temporarily very different thermodynamic properties which may create substantial driving forces for monomer migration which are absent in an uncontrolled polymerization.

Only when nonionic surfactants were used, miniemulsions were obtained that were stable throughout the polymerization. A number of controlled polymerizations were performed where the advantages of compartmentalized systems were exploited. Their relatively low termination rate allowed for the controlled preparation of low polydispersity homopolymers having a predetermined molar mass. Moreover, several methacrylate and styrene block copolymers were prepared with a much higher level of block purity than obtainable in typical solution polymerizations. Finally, it was shown that living radical polymerization could be conducted simultaneously with conventional radical polymerization, leading to a blend of latex particles with completely different characteristics. This novel process allows sophisticated materials engineering by a careful choice of reaction conditions.

The application of living polymerization in a miniemulsion with RAFT is still a relatively unexplored field. An understanding of the interaction of oligomers in general and dormant RAFT chains in particular with other emulsion components has not fully developed yet, but with the increasing attention that living polymerization systems are acquiring (particularly in dispersed media), major developments can be expected in the near future.

6.7. Experimental

Reagents: Monomers were obtained from Aldrich Chemicals. Before use they were distilled (except for EHMA) and passed through an inhibitor removal column (Aldrich – specific to the inhibitor type). 2,2'-Azobis[2-methyl-N-(2-hydroxyethyl)propionamide] (VA-086) and 1,1'-Azobis(1-cyclohexanecarbonitrile) (V-40) were obtained from Wako Chemicals and used without purification. 2,2'-azobisisobutyronitrile (AIBN, 98%) was purchased from Merck and recrystallized from methanol before use. Potassium persulfate (KPS), hexadecane (HD), potassium nitrodisulfonate (Fremy's salt), and sodium hydrogen carbonate were obtained from Aldrich. Sodium metabisulfite ($Na_2S_2O_5$, used as redox couple with KPS) and sodium dodecyl sulfate (SDS) were obtained from Fluka. Hydroquinone, used to quench gravimetric samples, was obtained from Merck. All were used as received. Kraton L-1203 (a monohydroxyl functional copolymer of ethylene and butylene $M_n \approx 4 \cdot 10^3$ g/mol, polydispersity ≈ 1.05) was received from Shell Chemicals.

The synthesis of 2-cyanoprop-2-yl dithiobenzoate (**1**, Scheme 6.2), 2-phenylprop-2-yl dithiobenzoate (**2**, Scheme 6.2) and 2-(ethoxycarbonyl)prop-2-yl dithiobenzoate (**3**, Scheme 6.2) is described in chapter 3. Polymeric RAFT agents were prepared by either organic procedures (**4**, Scheme 6.2) or solution polymerization (**5**, Scheme 6.2) of methyl methacrylate in the presence of **1** (Scheme 6.2). The preparation and characterization of **4** is described in chapter 3 and in reference 51. RAFT agent **5** has an apparent number average molar mass of $3.5 \cdot 10^3$ g/mol and a polydispersity of 1.07, determined by GPC against polystyrene standards.

Miniemulsion Procedure: Monomer was mixed with RAFT agent, hydrophobe and oil soluble initiator (AIBN, V-40, if applicable), comprising the preliminary organic-phase. This organic phase was mixed well until all contents were dissolved. While stirring vigorously (magnetic stirrer), the organic phase was dropwise added to a solution of the surfactant in water. The flask was left stirring to homogenize for 60 minutes after which a sonicating probe (400W, Dr. Hielscher UP400S) was immersed into this pre-emulsion. Stirring continued for 12 minutes while sonicating (amplitude 30%, cycle 1.0). 10–12 minutes was found to be the optimum duration of sonication for these recipes, leading to almost immediate polymerization after injection of initiator. When the pre-mixed emulsion was sonicated for roughly 30 minutes, retardation in the early stages of polymerization was observed. During this process, the miniemulsion was cooled by a water bath to keep its temperature below 20°C. The miniemulsion was then transferred into a three-necked

250ml round bottom flask equipped with reflux cooler and containing water-soluble initiator (potassium persulfate or VA-086, when applicable). The round bottom flask was then immersed into an oil bath, that had been pre-heated to the reaction temperature (70 °C) and polymerization was carried out under an argon atmosphere. During regular time intervals, samples were taken for particle size analyses by light scattering, gravimetric conversion measurement and GPC analyses.

Kinetic Analysis: Conversion of monomer to polymer was followed through dry-solids (gravimetric analysis). Samples were taken regularly throughout the polymerization, quenched with a few crystals of hydroquinone, and pre-dried on a hotplate at 60 °C, followed by drying in a vacuum oven at slowely increasing temperatures up to 120 °C.

GPC Analysis: GPC analyses were performed on a Waters system equipped with two PLgel Mixed-C columns, a UV and an RI detector. Reported molar masses are apparent values expressed in polystyrene equivalents. Although Mark-Houwink parameters were available for the polymers studied, a correction procedure was not applied, as its validity is only established for molar masses exceeding approximately 2.0×10^4 g/mol.

Conductivity Analysis: Conductivity of the continuous phase was measured by sampling as on-line probe tips were suspect to accumulate polymer that would give anomalous readings. Samples were taken from the reactor and immediately measured using a Radiometer Copenhagen CDM 80 conductivity meter (20 µS/cm to 2000 mS/cm).

HPLC Analyses: The HPLC analyses were performed using an Alliance Waters 2690 Separation Module. Detection was done using a PL-EMD 960 ELSD detector (Polymer Laboratories) and using a 2487 Waters dual UV detector at wavelengths of 254 and 320 nm. All samples were analyzed by injecting 10µl of a solution of the dried polymer in tetrahydrofuran at a concentration of 5 mg/ml. Columns were thermostated at 35 °C. Samples were analyzed on a NovaPak® CN column (Waters, 3.9×150 mm) by the application of a gradient from heptane to THF in 40 minutes. Data for both GPC and HPLC were acquired by Millennium 32 3.05 software.

Light Scattering: Particle diameters were determined by light scattering on a Malvern 4700. For this purpose, samples were diluted with water. Emulsion NI-6 was diluted with water saturated with styrene to preserve the original droplet size.

Electron Microscopy: A small film cast from the latex sample was vitrified by liquid ethane. Images were recorded on a Philips TEM (CM 12) at –120 °C. The advantage of cryogenic transmission electron microscopy is that staining of the latex is not nessecary and that the technique is readily applicable to polymers with a low glass transition temperature without changing the sample morphology.

6.8. References

1. taken from *She's lost control* by Joy Division on the album *Unknown Pleasures*, © Zomba Publishing / Fractured Music, **1979**
2. The work described in this chapter has been published elswhere in a slightly modified version. Miniemulsions stabilized by nonionic surfactants: De Brouwer, H.; Tsavalas, J. G.; Schork, F. J.; Monteiro, M. J. *Macromolecules* **2000**, *33*, 9239. Miniemulsions stabilized by ionic surfactants: Tsavalas, J. G.; Schork, F. J.; De Brouwer, H.; Monteiro, M. J. *Macromolecules* **2001**, in press.
3. Sudol, E. D.; El-Aasser, M. S. ; Lovell, P. A. and El-Aasser, M. S., Ed.: Chichester, 1997, p. 699
4. Gilbert, R. G. Emulsion Polymerization: A Mechanistic Approach; Academic: London, **1995**
5. Landfester, K.; Bechthold, N.; Forster, S.; Antonietti, M. *Macromol. Rapid Commun.* **1999**, *20*, 81
6. Landfester, K.; Bechthold, N.; Tiarks, F.; Antonietti, M. *Macromolecules* **1999**, *32*, 5222
7. Weiss, J.; McClements, D. J. *Langmuir* **2000**, *16*, 5879
8. Weiss, J.; Canceliere, C.; McClements, D, J. *Langmuir* **2000**, *16*, 6833
9. Webster, A. J.; Cates, M. E. *Langmuir* **1998**, *14*, 2068
10. Ugelstad, J.; Mørk, P. C.; Herder Kaggerud, K.; Ellingsen, T.; Berge, A. *Adv. Colloid Interface Sci.* **1980**, *13*, 101
11. Mouran, D.; Reimers, J.; Schork, F. J. *J. Polym. Sci. Part A: Polym. Chem.* **1996**, *34*, 1073
12. Chern, C. S.; Liou, Y. C.; Chen, T. J. *Macromol. Chem. Phys.* **1999**, *199*, 1315
13. Miller, C. M.; Blythe, P. J.; Sudol, E. D.; Silebi, C. A.; El-Aasser, M. S. *J. Polym. Sci. Part A: Polym. Chem.* **1994**, *32*, 2365
14. Blythe, P. J.; Morrison, B. R.; Mathauer, K. A.; Sudol, E. D.; El-Aasser, M. S. *Langmuir* **2000**, *16*, 898
15. Reimers, J.; Schork, F. J. *J. Appl. Polym. Sci.* **1996**, *59*, 1833
16. Reimers, J. L.; Schork, F. J. *J. Appl. Polym. Sci.* **1996**, *60*, 251
17. Choi, Y. T.; Sudol, E. D. Vanderhoff, J. W.; El-Aasser, M. S. *J. Polym. Sci. Polym. Chem. Ed.* **1985**, *23*, 2973
18. Reimers, J.; Schork, F. J. *J. Appl. Polym. Chem.* **1995**, *33*, 1391
19. Prodpran, T.; Dimonie, V. L.; Sudol, E. D.; El-Aasser, M. S. *Macromol. Symp.* **2000,** *155*, 1
20. Matyjaszewski, K.; Shipp, D. A.; Qiu, J.; Gaynor, S. G. *Macromolecules* **2000,** *33*, 2296
21. Farcet, C.; Lansalot, M.; Charleux, B.; Pirri, R.; Vairon, J. P. *Macromolecules* ASAP
22. Charleux, B. *Macromolecules* **2000**, *33*, 5358
23. Butté, A.; Storti, G.; Morbidelli, M. *Macromolecules* **2000**, *33*, 3485
24. Lansalot, M.; Farcet, C.; Charleux, B.; Vairon, J.-P.; Pirri,R. *Macromolecules* **1999**, *32,* 7354
25. Farcet, C.; Lansalot, M.; Pirri, R.; Vairon, J. P.; Charleux, B. *Macromol. Rapid Commun.* **2000**, *21*, 921
26. Kanagasabapathy, S.; Claverie, J.; Uzulina I. *Polym. Prepr.* **1999**, *218*, 422
27. Uzulina I.; Kanagasabapathy, S.; Claverie, J. *Macromol. Symp.* **2000**, *150*, 33
28. Monteiro, M. J.; Sjöberg, M.; Van der Vlist, J.; Göttgens, C. M. *J. Polym. Sci. Part A: Polym. Chem.* **2000**, *38*, 4206
29. Monteiro, M. J.; Hodgson, M.; De Brouwer, H. *J. Polym. Sci. Part A: Polym. Chem.* **2000**, *38*, 3864
30. Hodgson, M. *Masters thesis* **2000** University of Stellenbosch, South Africa
31. Le, T. P.; Moad, G.; Rizzardo, E.; Thang, S. H. Patent WO 98/01478 (1998) [*Chem. Abstr.* **1998**,

128:115390]
32. Moad, G.; Chiefari, J.; Chong, Y. K.; Krstina, J.; Mayadunne, R. T. A.; Postma, A.; Rizzardo, E.; Thang, S. H. *Polymer International* **2000**, *49*, 993
33. Lichti, G.; Sangster, D. F.; Whang, B. C. Y.; Napper, D. H.; Gilbert, R. G. *J. Chem. Soc. Faraday Trans. I* **1982**, *78*, 2129
34. Morrison, B. R.; Casey, B. S.; Lacík, I.; Leslie, G. L.; Sangster, D. F.; Gilbert, R. G.; Napper, D. H. *J. Polym. Sci. A: Polym. Chem.* **1994**, *32*, 631
35. Monteiro, M. J.; de Brouwer, H. *Macromol. Rapid Commun.* submitted.
36. Maeder, S.; Gilbert, R. G. *Macromolecules* **1998**, *31*, 4410
37. Goto, A.; Sato, K.; Fukuda, T.; Moad, G.; Rizzardo, E.; Thang, S. H. Polymer Preparations **1999**, *40*, 397
38. Buback, M.; Gilbert, R. G.; Hutchinson, R. A.; Klumperman, B.; Kuchta, F.-D.; Manders, B. G.; O'Driscoll, K. F.; Russell, G. T.; Schweer, *J. Macromol. Chem. Phys.* **1995**, *196*, 3267
39. Note that the initial concentration of initiator $[I]_0$ should be based on the same volume as $[M]_0$ and $[RAFT]_0$ and that the volume cancels out by the devision. Therefore these concentrations may be replaced by molar amounts. $[I]_w$ and $[M]_w$ are the actual concentrations of initiator and monomer in the water phase.
40. Müller, A. H. E.; Zhuang, R.; Yan, D.; Litvenko, G. *Macromolecules* **1995**, *28*, 4326
41. van Herk, A. M. *J. Macromol. Sci., Rev. Macromol. Chem. Phys.* **1997**, *C37*, 633
42. de Brouwer, H.; Tsavalas, J. G.; Schork, F. J.; Monteiro, M. J. *Macromolecules* in press
43. Fontenot, K.; Schork, F. J. *J. Appl. Polym. Sci.* **1993**, *49*, 633
44. Noël, L. F. J.; Janssen, R. Q. F.; van Well, W. J. M.; van Herk, A. M.; German, A. L. *J. Colloid & Interface Sci.* **1995**, *175*, 461
45. Blackley, D. C.; Haynes, A. C. J. Chem. Soc., *Faraday Trans. 1* **1979**, *75*, 935
46. Charmot, D.; Corpart, P.; Adam, H.; Zard, S. Z.; Biadatti, T.; Bouhadir, G. *Macromol. Symp.* **2000**, *150*, 23
47. Hoffman, B. Controlled radical polymerization using RAFT; Eindhoven University of Technology: Eindhoven, **2000**
48. Landfester, K.; Bechthold, N.; Tiarks, F.; Antonietti, M. *Macromolecules* **1999,** *32*, 2679
49. Chern, C.-S.; Liou, Y.-C. *Macromol. Chem. Phys.* **1998**, *199*, 2051
50. Van Herk, A in *Polymeric dispersions: principles and applications*, Asua, J. M. (Ed.) NATO ASI Series E, Applied Sciences **1997**, *335*, 17
51. De Brouwer, H.; Schellekens, M. A. J.; Klumperman, B.; Monteiro, M, J.; German, A. L. *J. Polym. Sci. Part A: Polym. Chem.* **2000**, *38*, 3596